Journal of
Medicinal Chemistry

Article

Design and Discovery of an Orally Efficacious Spiroindolinone-based Tankyrase Inhibitor for the Treatment of Colon Cancer

Fumiyuki Shirai, Anna Mizutani, Yoko Yashiroda, Takeshi Tsumura, Yuko Kano, Yukiko Muramatsu, Tsubasa Chikada, Hitomi Yuki, Hideaki Niwa, Shin Sato, Kenichi Washizuka, Yasuko Koda, Yui Mazaki, Myung-Kyu Jang, Haruka Yoshida, Akiko Nagamori, Masayuki Okue, Takashi Watanabe, Kouichi Kitamura, Eiki Shitara, Teruki Honma, Takashi Umehara, Mikako Shirouzu, Takehiro Fukami, Hiroyuki Seimiya, Minoru Yoshida, and Hiroo Koyama

J. Med. Chem., **Just Accepted Manuscript** • DOI: 10.1021/acs.jmedchem.0c00045 • Publication Date (Web): 23 Mar 2020

Just Accepted

is published by the American Chemical Society. 1155 Sixteenth Street N.W., Washington, DC 20036

	Division, Pharmaceutical Research Center Honma, Teruki; RIKEN Yokohama Branch , Center for Life Science Technologies Umehara, Takashi; Institute of Physical and Chemical Research, Center for Biosystems Dynamic Research Shirouzu, Mikako; RIKEN Center for Life Science Technologies , Fukami, Takehiro; RIKEN Program for Drug Discovery and Medical Technology Platforms Seimiya, Hiroyuki; Public Interest Incorporated Foundation Japanese Foundation for Cancer Research, Divisoin of Molecular Biotherapy, Cancer Chemotherapy Center Yoshida, Minoru; RIKEN Center for Sustainable Resource Science, Synthetic Organic Chemistry Laboratory Koyama, Hiroo; RIKEN Center for Sustainable Resource Science, Drug Discovery Chemistry Platform Unit

Design and Discovery of an Orally Efficacious Spiroindolinone-based Tankyrase Inhibitor for the Treatment of Colon Cancer

Fumiyuki Shirai,[*†] *Anna Mizutani,*[‡‡] *Yoko Yashiroda,*[‡] *Takeshi Tsumura,*[#] *Yuko Kano,*[#] *Yukiko Muramatsu,*[‡‡] *Tsubasa Chikada,*[¶] *Hitomi Yuki,*[∥] *Hideaki Niwa,*[⊥] *Shin Sato,*[⊥] *Kenichi Washizuka,*[†] *Yasuko Koda,*[†] *Yui Mazaki,*[‡] *Myung-Kyu Jang,*[‡‡,§§] *Haruka Yoshida,*[‡‡] *Akiko Nagamori,*[‡‡] *Masayuki Okue,*[††] *Takashi Watanabe,*[#] *Kouichi Kitamura,*[▽] *Eiki Shitara,*[○] *Teruki Honma,*[∥] *Takashi Umehara,*[⊥] *Mikako Shirouzu,*[⊥] *Takehiro Fukami,*[§] *Hiroyuki Seimiya,*[‡‡,§§] *Minoru Yoshida,*[‡,§§§] *and Hiroo Koyama*[*,†]

†Drug Discovery Chemistry Platform Unit; ‡Chemical Genomics Research Group, RIKEN Center for Sustainable Resource Science; §RIKEN Program for Drug Discovery and Medical Technology Platforms, 2-1 Hirosawa, Wako, Saitama 351-0198, Japan

// Drug Discovery Computational Chemistry Platform Unit; ⊥Drug Discovery Structural Biology Platform Unit, RIKEN Center for Biosystems Dynamics Research, 1-7-22 Suehiro-cho, Tsurumi-ku, Yokohama, Kanagawa 230-0045, Japan

#Medicinal Chemistry Laboratory; ¶Pharmacokinetics and Analysis Laboratory; ▽ Pharmacology Research Laboratory; ○Pharmaceutical Research Division, Pharmaceutical Research Center; ††Process Chemistry Laboratory, Manufacturing & Control Research Labs, Meiji Seika Pharma Co., Ltd., 760 Morooka-cho, Kohoku-ku, Yokohama, Kanagawa 222-8567, Japan

‡‡Division of Molecular Biotherapy, Cancer Chemotherapy Center, Japanese Foundation for Cancer Research, 3-8-31 Ariake, Koto-ku, Tokyo 135-8850, Japan

§§Department of Computational Biology and Medical Sciences, Graduate School of Frontier Sciences, The University of Tokyo, 3-8-31 Ariake, Koto-ku, Tokyo 135-8850, Japan

§§§Department of Biotechnology, The University of Tokyo, 1-1-1 Yayoi, Bunkyo-ku, Tokyo 113-8657, Japan

KEYWORDS: tankyrase, Wnt/β-catenin signaling, AXIN, β-catenin, spiroindoline, spiroindolinone, pharmacokinetics, P-glycoprotein efflux, mouse xenograft model

ABSTRACT: Tankyrases (TNKS/TNKS2) belong to the poly(ADP-ribose) polymerase family. Inhibition of their enzymatic activities attenuates the Wnt/β-catenin signaling, which plays an important role in cancer pathogenesis. We previously reported the discovery of RK-287107, a spiroindoline-based, highly selective, potent tankyrase inhibitor. Herein we describe the optimization process of RK-287107 leading to RK-582, which exhibits a markedly improved robust tumor growth inhibition in a COLO-320DM mouse xenograft model when orally administered. In addition to the dose-dependent elevation and attenuation of the levels of biomarkers AXIN2 and β-catenin, respectively, results of the TCF reporter and cell proliferation studies on COLO-320DM are discussed.

■ INTRODUCTION

Globally, colorectal cancer (CRC) is the third most common cause of cancer deaths in men and the second in women.[1] Over 90% of CRC cases have been reported to accompany with a hyper-activated WNT signaling pathway. Moreover, loss-of-function mutations of the tumor suppressor adenomatous polyposis coli (APC) [2,3] are found in approximately 80% of the cases. Tankyrases (tankyrase-1/TNKS/TNKS1/PARP5a and tankyrase-2/TNKS2/PARP5b) are members of the poly(ADP-ribose) polymerases (PARPs) and possess PARP catalytic domains. Tankyrase-1 and tankyrase-2 are reported to be functionally redundant.[4]

Tankyrases add multiple ADP-ribose moieties (PARsylate) to various target proteins, including AXIN, which is a negative regulator of the WNT signaling pathway. PARsylated AXIN undergoes ubiquitin-dependent degradation in the proteasomes, leading to the translocation of β-catenin to the nucleus and activation of the WNT signaling pathway.

In 2009, Huang et al. reported that inhibition of the tankyrase enzymatic activity by XAV939 attenuates the WNT signaling via AXIN stabilization. In addition, XAV939 inhibits colony formation of APC-mutant CRC cells (DLD-1 cells).[5] Recent reports

indicate that tankyrase inhibitors suppress CRC with truncated APC in *in vivo* and *ex vivo* mouse models as well as patient-derived cell lines.[6,7] These findings provided important insights to the therapeutic utility of tankyrase inhibitors to treat cancer harboring aberrant Wnt/β-catenin signaling.

Since tankyrases possess highly divergent functions, including regulation of the WNT/β-catenin pathway,[5] telomere elongation,[8] Hippo pathway,[9] mitotic checkpoint,[10] and vesicle trafficking,[11] they have attracted significant interest as molecular targets for cancer treatment.[12-14] To date, X-ray crystallographic studies have identified three different binding motifs: 1) an adenosine pocket binder such as IWR-1 (**2**),[15] IWR-2 (**3**)[16] and G007-LK (**4**),[17] 2) a nicotinamide pocket binder such as XAV-939 (**5**)[18,19] and RK-287107 (**1**),[20,21] and 3) a dual pocket binder such as NVP-TNKS656 (**6**)[22] (Figure 1).

An important issue in cancer drug development is the balance between efficacy and toxicity. In a 2013 report, the antitumor activity and the intestinal toxicity of G007-LK, an adenosine pocket binder, were carefully studied in a xenograft model.[23] Although G007-LK showed potent tumor growth inhibition in APC-mutant CRC cell lines (COLO-320DM and SW403) mouse xenograft models, dose-limiting epithelial degeneration and a

reduction of crypt proliferation in the small intestine were observed among the mice treated for 21 days.[23] In addition, a recent report demonstrated that tankyrase inhibitor G-631 (**7**), a nicotinamide pocket binder, caused dose-dependent intestinal toxicity in mice while showing modest antitumor effects in a SW403 xenograft model at 100 mg/kg daily oral dosing. Based on these findings, they concluded that the clinical utility of orally administered tankyrase inhibitors would be limited due to the "on-target" intestinal toxicity.[24]

We recently discovered a tetrahydroquinazoline-based potent tankyrase inhibitor RK-287107 (**1**), which shows >200-fold selectivity against other PARP enzymes and modest antitumor effects in a mouse xenograft model without notable weight loss.[20] Given that multiple binding motifs of tankyrase inhibitors have been reported and that previously reported tankyrase inhibitors showed variable levels of anticancer effects and intestinal toxicity, we decided to find tankyrase inhibitors with a reasonable therapeutic window.

Herein we describe the design and discovery of an orally bioavailable, potent and novel tankyrases RK-582. RK-582 exhibits robust tumor growth inhibitory activity in a mouse COLO-320DM xenograft model either with oral or intraperitoneal administration.

RK-582 possesses an excellent pharmacokinetic profile and exhibits a comparable level of efficacy with RK-287107, at a much lower dose. Concomitant measurements of the biomarker levels revealed dose-dependent attenuation of active β-catenin and elevation of AXIN2, clearly indicating the inhibition of WNT signaling.

■ RESULTS AND DISCUSSION

Chemistry. Scheme 1 depicts synthesis of tetrahydroquinazolinone analogues. 8-Methylquinazoline compounds **8** and **9** were synthesized in one step with good yields via a substitution reaction between 2-chloro-8-methylquinazolin-4(3*H*)-one (**17**)[25] and 1-hydroxyethylspiroindoline or 1-hydroxyethylspiroindolinone intermediates (**20** or **21**), [21] respectively. 8-Methyltetrahydropyridopyrimidinone compounds **10** and **11** were synthesized in three steps in good yields via a substitution reaction between 2-chloropyrido[2,3-*d*] pyrimidin-4(3*H*)-one (**18**)[26] and **20** or **21**, respectively, methylation of the pyridine moiety, and hydrogenation with platinum oxide. Pyrrolopyrimidinone compounds **12** and **13** were prepared via a substitution reaction between 2-chloro-7-methyl-3,7-dihydro-4*H*-pyrrolo[2,3-*d*]pyrimidin-4-one (**19**)[27] and **20** or **21**, respectively.

Dihydropyrrolopyrimidinone compounds **14** and **15** were prepared by hydrogenation of **12** or **13**, respectively.

Scheme 2 outlines the synthesis of 1-substituted spiroindolinone derivatives. Following the same or a slightly modified procedure of Scheme 1, 1-methyl substituted spiroindolinone derivative **11a** was synthesized in three steps in a moderate yield from 2-chloropyrido[2,3-*d*] pyrimidin-4(3*H*)-one (**18**) and 1-methyl spiro-intermediate **21a**, which was prepared by the published procedure.[21] Compounds (**11b–h**) were synthesized efficiently in one step via a substitution reaction between 2-chloro-8-methyl-5,6,7,8-tetrahydropyrido[2,3-*d*]pyrimidin-4(3*H*)-one (**28**), which was prepared from **18** in four steps, and spiro-intermediates (**21b–h**) prepared from **24** by the published procedure.[21]

Scheme 3 outlines the synthesis of 6-oxysubstituted spiroindolinone derivatives. Following the same procedure as described above, compounds (**37a–j**) were synthesized from the intermediate **28** and spiro-intermediates (**36a–j**) in one step. To synthesize the spiro-intermediates (**36a–j**), regioselective 6-substituted spiro-3-piperidinylindolinone formation was the key step. *tert*-Butyl 1-methyl-2-oxospiro[indoline-

3,4'-piperidine]-1'-carboxylate (**33**) was obtained by 1) *gem*-bis alkylation of 2-(2,6-difluoro-4-methoxyphenyl)acetonitrile, which was prepared from palladium coupling between 2-bromo-1,3-difluoro-5-methoxybenzene and *tert*-butyl 2-cyanoacetate, and decarboxylation of *tert*-butylcarboxylate, piperidine ring cyclization using Boc-bis(chloroethyl)amine to provide a piperidine-4-carbonitrile (**31**), 2) subsequent hydrolysis of the nitrile group, 3) nucleophilic aromatic substitution to form a indolinone and methylation of the 1-NH position of the indolinone to furnish **33**. Spiroindolinone precursors (**36b–j**) were obtained by demethylation of 6-methoxy group of **33** using boron tribromide, restoration of the Boc group (**34**), and introduction of R groups via an alkylation (**36b** and **36j**) or a Mitsunobu reaction (**36c**–**i**) followed by the deprotection of the Boc group.

Syntheses of the 6-aminosubstituted spiroindolinone analogs with various saturated heterocyclic substituents were accomplished with the procedure outlined in Scheme 4. Compounds (**41a–g**) were synthesized from the intermediate **28** and spiro-intermediates (**40a–g**) by the same procedure as described above. Spiro-intermediates (**40b–g**) were prepared by palladium coupling between cyclic amines and an intermediate **38**, which

was prepared from **34** and triflic anhydride, and deprotection of the Boc group. The spiro-intermediate **40a** was prepared by palladium coupling between dimethylamine hydrochloride and an intermediate **42** followed by deprotection of the Cbz group.

SAR of analogs beyond the tetrahydroquinazolinone structure. Recently discovered RK-287107 (**1**), which is a nicotinamide pocket binder, exhibits potent TNKS/TNKS2 enzyme inhibitory activities with an excellent selectivity against other PARP family enzymes (PARP1, PARP2, and PARP10) as well as TCF reporter activity in HEK293 and DLD-1cells, and cell proliferation of COLO-320DM cells.[21] However, the relatively high doses of **1** required during the xenograft study prompted us to search for compounds with significantly improved cell growth inhibition, a 50% growth inhibition value (GI_{50}) of <0.3 μM, and efficacy against tumor proliferation in a mouse xenograft model.[20]

We prepared various nicotinamide pocket binders, including the derivatives of 8-methylquinazolin-4(3*H*)-one (**8** and **9**), 8-methyl-5,6,7,8-tetrahydropyrido[2,3-*d*]pyrimidin-4(3*H*)-one (MTPP) (**10** and **11**), 7-methyl-3,7-dihydro-4*H*-pyrrolo[2,3-*d*]pyrimidin-4-one (**12** and **13**) and 7-methyl-3,5,6,7-tetrahydro-4*H*-pyrrolo[2,3-

d]pyrimidin-4-one (**14** and **15**). Compared to **1**,[20] the enzyme inhibitory activities of these newly synthesized compounds are maintained or improved (Table 1). In addition, compound **10** and **11**, derivatives with the MTPP moiety, possess improved activities in both the cellular TCF reporter and cell proliferation assays. These compounds, exhibiting the similar TNKSs inhibitory and improved cell growth inhibitory activities with a GI_{50} value of 0.25 μM when compared to **1**, suggested that the introduction of the MTPP moiety may improve the ability of cellular penetration. Table 2 summarizes the results of physicochemical studies and liver microsomal stability for **10** and **11**, and indicated that PAMPA values of **10** and **11** were almost same as that of **1**. These findings seem to suggest that an increase in the cellular permeability of those compounds with MTPP moiety does not come from increased lipid membrane permeability, but other factor(s) influencing an ability of cellular penetration.

Although the human and mouse liver microsomal stabilities of **10** and **11** need to be improved, the slightly superior *in vitro* activities, aqueous solubility, free fraction ratio in blood plasma and microsomal stability of spiroindolinone **11** caught our attention. Hence, we focused on the indolinone derivatives with the MTPP moiety for further

optimization.

Table 1. SAR study of analogs of the tetrahydroquinazolinone moiety.

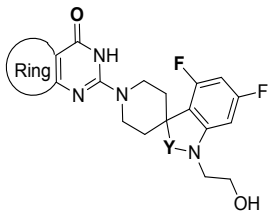

Cmpd	Ring	Y	Enzyme IC_{50} (nM)[a]		TCF reporter IC_{50} (nM)[b]		COLO-320DM GI_{50} (μM)[c]
			TNKS	TNKS2	HEK293	DLD-1	
1	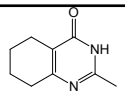	CH_2	14.3	10.6	12.1	77.6	1.63
7		C=O	14.9	20.6	2.1	71.2	2.27
8	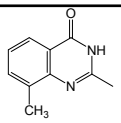	CH_2	5.5	8.5	3.1	13.7	0.72
9		C=O	5.3	3.4	0.2	4.8	2.49
10	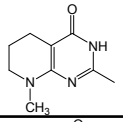	CH_2	13.6	21.4	2.7	7.0	0.25
11		C=O	7.5	13.5	1.1	3.9	0.25
12	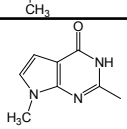	CH_2	3.8	7.0	1.1	7.1	3.56
13		C=O	4.5	10.2	1.5	6.3	>20.0
14	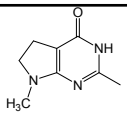	CH_2	53.5	73.6	36.5	140.6	5.01
15		C=O	14.1	27.6	4.4	32.9	2.37

[*a*] Mean values are shown from two independent experiments conducted in duplicate.

[*b*] Mean values are shown from two independent experiments conducted in triplicate.

[*c*] COLO-320DM growth inhibition was evaluated by the CellTiter-Glo cell viability assay method. Three independent experiments were conducted in triplicate.

Table 2. ADME properties of 8-methyl-5,6,7,8-tetrahydropyrido[2,3-*d*]pyrimidin-4(3*H*)-one derivatives (10 and 11).

Compound		**1** 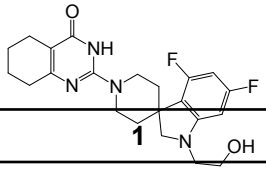	**10** 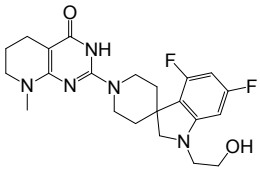	**11** 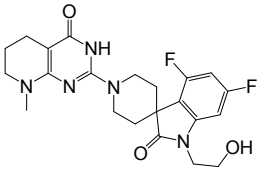
Aqueous solubility (pH7.4 PBS; μg/mL)		72.1	40.2	82.9
PAMPA (4 h; x 10^{-6} cm/s)		2.0	3.3	3.0
Microsomal stability: 30min / 60min (Remaining %)	Mouse	18.3 / 3.2	0.3 / 0.2	21.2 / 8.5
	Rat	12.8 / 3.2	0.4 / 0.2	2.0 / 0.5
	Human	5.9 / 2.2	7.4 / 1.4	21.0 / 6.3
Protein binding[a] (Human, Mouse; % free)		Hu: 1.5%, Mo:0.4%	Hu: 0.5%, Mo: 0.2%	Hu: 2.2%, Mo: 8.3%

[*a*] Human (Hu) /Mouse (Mo) plasma protein binding, % value of the free fraction of the compound.

SAR of the right side spiroindolinone substructure. Analysis of the effects of the substitution pattern on the spiroindoline moiety in our previous study indicated that 4-halo substituents, especially 4-fluoro substituent (R^2 = F), provide the most potent enzyme, cellular TCF reporter, and cell growth inhibitory activities.[21] The addition of a 5-

substituent (R^3) attenuates the inhibitory activity, presumably due to the destabilizing effect by steric repulsion between the 5-substituent and Pro1034 and Gly1074 residues of tankyrase-2 (data not shown). In contrast, our previous study also suggested the addition of 1, 6, and 7-substituents (R^1, R^4, and R^5, respectively) would have little adverse effect on the enzyme inhibitory activity, because the direction of these substituents is toward cytosolic space of the enzyme. However, such an addition should exert various effects on the drug-like properties (e.g. aqueous solubility and microsomal stability etc.). Thus, we investigated the structure-activity relationship of the MTPP derivatives with substituents at the 1- and 6-position (R^1 and R^4, respectively) on the spiroindolinone moiety (Figure 2).

SAR of the 1-substituted spiroindolinone series. Initially, we focused on the effects of the substituent at the 1-position (R^1) of the indolinone (Table 3). All the 1-substituted spiroindolinone derivatives except **11g** predictably show the comparable enzymatic and cellular activities as **11**. The aqueous solubility increases for substituents containing hydroxyl (**11** and **11h**), nitrile (**11d**), and carboxymethyl (**11g**) groups. Only compounds **11g** and **11h** show improved aqueous solubility and microsomal stability. However, the

P-glycoprotein (P-gp) efflux ratio of the compounds containing hydroxyl (**11** and **11h**), nitrile (**11d**), sulfone (**11e**) or oxetane (**11f**) increases to more than eight as measured by a cell system method, which involves MDR1 overexpressing MDCKII cells (MDCKII-MDR1). In particular, the efflux ratio (ER) of **11h** is extremely high (ER = 43.7). Although **11g** shows superior *in vitro* profiles, including aqueous solubility and microsomal stability, and P-gp efflux activity, its TCF reporter (HEK293 and DLD-1 IC_{50}: 221 and 1185 nM, respectively) and cell growth inhibitory (GI_{50}: 12.6 μM) activities are substantially lower, presumably due to its low cellular permeability. Based on these findings, further optimizations were performed with derivatives with the 1-methyl moiety. We comprehensively preferred this moiety on account of the balance of biological activities and drug-like properties such as solubility and P-gp efflux activity. Next we shifted our focus to the substituent at the 6-position of the spiroindolinone derivatives.

Table 3. SAR development of 1-substituted spiroindolinone series.

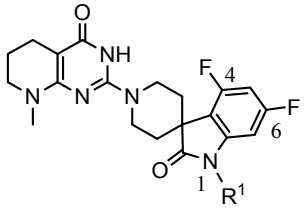

Cmpd	R^1	Enzyme IC_{50} (nM)[a]		TCF reporter IC_{50} (nM)[b]		COLO-320DM GI_{50} (μM)[c]	Aq.Sol.[d] (pH7.4, μg/mL)	Hu/Mo Mic.Stab.[e] (% @ 60 min)	P-gp ER[f] MDCK-MDR1 + / - (NER)
		TNKS	TNKS2	HEK293	DLD-1				
11	CH_2CH_2OH	7.5	13.5	1.1	3.9	0.25	82.9	6.3 / 2.0	24.6 / 6.4 (3.8)
11a	CH_3	7.9	10.7	3.9	14.4	0.22	16.0	0.3 / 0.0	3.1 / 1.1 (2.8)
11b	CH_2CH_2OMe	10.3	11.7	0.3	3.0	0.05	6.3	1.8 / 0.1	4.8 / 1.3 (3.7)
11c	CH_2CF_3	16.2	32.4	0.2	2.4	0.07	1.3	8.0 / 1.0	2.0 / 0.7 (2.9)
11d	CH_2CN	3.7	6.1	0.2	1.6	0.44	50.5	6.1 / 1.2	11.7 / 2.3 (5.1)
11e	CH_2SO_2Me	4.3	5.5	0.1	5.7	0.53	3.0	4.1 / 0.1	12.0 / 3.3 (3.6)
11f		7.8	12.2	0.3	7.2	0.20	9.3	0.0 / 0.3	8.4 / 1.2 (7.0)
11g	CH_2COOH	28.5	29.8	221	1185	12.6	92.1	100 /100	0.5 / 0.4 (1.3)
11h	$CH_2CHOHCH_2OH$	8.9	12.5	0.7	14.5	0.71	88.2	23.9 / 42.7	43.7 /11.2 (3.9)

[*a*] Mean values are shown from two independent experiments conducted in duplicate.

[*b*] Mean values are shown from two independent experiments conducted in triplicate.

[*c*] COLO-320DM growth inhibition was evaluated by the CellTiter-Glo cell viability assay method. Three independent experiments were conducted in triplicate. [*d*] Aq.Sol.: Aqueous solubility in pH 7.4 phosphate buffer. [*e*] Hu/Mo Mics.Stab.: Liver microsomal

stability was determined by the remaining % of compound after 60 min of incubation with human (Hu) or mouse (Mo) liver microsome according to the protocol described in our previous report.[21] [*f*] P-gp ER MDCK-MDR1+ / - : Efflux ratio (ER: $Papp_{BtoA}/Papp_{AtoB}$) of MDR1 overexpressing MDCKII (+) or wild-type MDCKII (-) cells was determined. Net efflux ratio (NER) was calculated as the ratio of the value of MDCKII-MDR1 to MDCKII.

Effects of 6-alkoxy substituents of the spiroindolinone series. Table 4 summarizes the *in vitro* activities and ADME profiles of compounds with various substituents at the 6-position of the indolinone ring. Replacement of the 6-fluoro group (R^4) of **11a** with substituted methoxy groups improves or maintains the enzyme, cellular TCF reporter and cell growth inhibitory activities (**37a–i**). In contrast, the TCF reporter inhibitory activity of **37j**, which possesses a carboxymethoxy moiety, is reduced, presumably by the poor cellular permeability. Surprisingly **37j** maintains the cell growth inhibitory activity with a GI_{50} value of 0.3 μM. To confirm whether this phenomenon is caused by tankyrase inhibition or not, we investigated the protein expression levels of AXIN2 and β-catenin, which are biomarkers of Wnt/β-catenin signaling. Given that the biomarker levels and cell growth inhibitory activity are not well correlated with each other, other mechanisms may be involved (Supporting Information Figure S1).

From the viewpoint of ADME properties, **37b**, which has a 2-hydroxyethoxy group, exhibits an improved aqueous solubility, but unfortunately indicates the poor microsomal stability and elevated P-gp efflux activity. Compounds (**37d–i**), which are substituted with a basic amino group, show excellent aqueous solubility and microsomal stability,

while the P-gp efflux liability deteriorates.

Table 4. Effects of 6-alkoxy substituents of the spiroindolinone series.

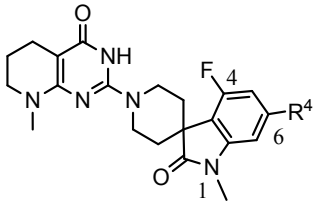

cmpd	R^4	Enzyme IC_{50} (nM)[a]		TCF reporter IC_{50} (nM)[b]		COLO-320DM GI_{50} (μM)[c]	Aq.Sol.[d] (pH7.4, μg/mL)	Hu/Mo Mic.Stab.[e] (% @ 60 min)	P-gp ER[f] MDCK-MDR1 + / - (NER)
		TNKS	TNKS 2	HEK293	DLD-1				
37a	$-OCH_3$	4.4	6.2	0.2	4.5	0.13	4.8	1.9 / 0.0	2.7 / 1.1 (2.5)
37b	$-OCH_2CH_2OH$	3.5	4.7	0.8	2.3	0.16	75.1	19.8 / 0.7	14.9 / 6.2 (2.4)
37c	$-OCH_2CH_2OCH_3$	4.8	6.4	0.1	1.3	0.05	11.4	1.8 / 13.7	7.5 / 2.1 (3.6)
37d	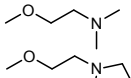	4.9	11.1	0.3	6.1	0.81	95.0	54.4 / 83.7	22.7 / 9.2 (2.5)
37e		11.1	12.4	0.4	6.6	1.08	100.1	61.5 / 100	21.9 / 7.1 (3.1)
37f	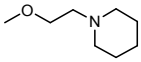	12.0	33.3	2.5	5.0	1.09	100.7	18.5 / 56.0	6.1 / 3.2 (1.9)
37g	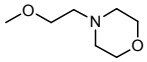	9.2	17.1	0.3	2.8	0.33	101.1	1.5 / 41.4	29.1 / 5.1 (5.7)
37h	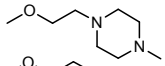	7.9	18.7	1.2	6.3	0.74	188.0	56.5 / 83.5	86.4 / 13.1 (6.6)
37i	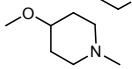	6.1	21.2	0.1	2.7	0.66	102.5	22.4 / 60.3	11.7 / 4.6 (2.5)
37j	$-OCH_2CO_2H$	4.2	9.9	507	1877	0.30	98.4	97.6 / 93.3	0.3 / 0.3 (1.0)

[*a*] Mean values are shown from two independent experiments conducted in duplicate.

[*b*] Mean values are shown from two independent experiments conducted in triplicate.

[*c*] COLO-320DM growth inhibition was evaluated by the CellTiter-Glo cell viability assay method. Three independent experiments were conducted in triplicate. [*d*] Aq.Sol.:

Aqueous solubility in a pH 7.4 phosphate buffer. [*e*] Hu/Mo Mics.Stab.: Human/mouse liver microsomal stability. [*f*] P-gp ER MDCK-MDR1+ / - : Efflux ratio (ER: $Papp_{BtoA}/Papp_{AtoB}$) of MDR1 overexpressing MDCKII (+) or wild-type MDCKII (-) cells was determined. Net efflux ratio (NER) was calculated as the ratio of the value of MDCKII-MDR1 to MDCKII.

Effects of 6-amino substituents of the spiroindolinone series. Table 5 summarizes the results of the SAR studies of compounds with various saturated heterocycle substituents at the 6-position of the indolinone moiety.

The enzyme (IC_{50} = 7–40 nM) and TCF reporter (0.1–30 nM) inhibitory activities can tolerate with the introduction of a saturated heterocyclic moiety at the 6-position, displaying the improved cell proliferation inhibitory activity (GI_{50} : <1.2 μM) and the acceptable aqueous solubility (**41c**–**g**) when compared to **1**. Compounds **41a** and **41b** show the good enzyme and TCF reporter inhibitory activities, and the acceptably low P-gp efflux ratios, but disappointingly exhibited the poor aqueous solubility and microsomal stability. Compounds (**41c**–**e** and **41g**) exhibited the moderate stability in human and mouse liver microsomes. But compounds (**41c**, **41d**, and **41e**) with basic

amino groups (pKa: >7.5) and **41f** with a 4-morpholinyl moiety show the moderate to high P-gp efflux ratio.

Compound **41g** with a 2,6-dimethylmorpholine moiety at the 6-position, shows the excellent P-gp efflux activity, improved microsomal stability and aqueous solubility. Compared to unsubstituted morpholine compound **41f**, the P-gp efflux ratio (MDCK-MDR1) of **41g** is dramatically decreased from 7.8 to 1.0 due to the introduction of two methyl groups on the morpholine moiety.

Table 5. Effects of 6-amino substituents of the spiroindolinone series.

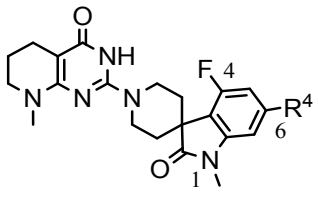

cmpd	R^4	Enzyme IC_{50} (nM)[a]		TCF reporter IC_{50} (nM)[b]		COLO-320DM GI_{50} (μM)[c]	Aq.Sol.[d] (pH7.4, μg/mL)	Hu/Mo Mic.Stab.[e] (% @ 60 min)	P-gp ER[f] MDCK-MDR1 + / - (NER)
		TNKS	TNKS 2	HEK293	DLD-1				
41a		6.3	13.0	4.6	20.7	1.17	7.4	1.8 / 1.8	2.7 / 1.1 (2.5)
41b		21.3	49.1	0.7	6.4	0.30	5.0	1.5 / 10.5	2.3 / 1.0 (2.3)
41c	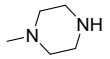	12.8	23.4	3.2	29.1	1.12	97.3	28.6 / 63.7	9.1 / 6.8 (1.3)
41d	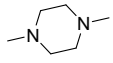	7.7	12.3	0.9	8.4	0.19	94.5	30.5 / 54.5	13.2 / 3.1 (4.3)
41e	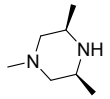	11.1	20.2	0.1	4.3	0.85	102.1	33.0 / 82.7	23.1 / 6.2 (3.7)
41f		14.9	10.5	0.1	2.0	0.10	72.2	6.3 / 46.5	7.8 / 1.9 (4.1)
41g	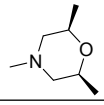	36.1	39.2	0.3	3.1	0.23	34.1	28.7 / 55.9	1.0 / 0.9 (1.1)

[*a*] Mean values are shown from two independent experiments conducted in duplicate.

[*b*] Mean values are shown from two independent experiments conducted in triplicate.

[*c*] COLO-320DM growth inhibition was evaluated by the CellTiter-Glo cell viability assay method. Three independent experiments were conducted in triplicate. [*d*] Aq.Sol.:

Aqueous solubility in a pH 7.4 phosphate buffer. [*e*] Hu/Mo Mics.Stab.: Human/mouse liver microsomal stability. [*f*] P-gp ER MDCK-MDR1+ / - : Efflux ratio (ER: $Papp_{BtoA}/Papp_{AtoB}$) of MDR1 overexpressing MDCKII (+) or wild-type MDCKII (-) cells was determined. Net efflux ratio (NER) was calculated as the ratio of the value of MDCKII-MDR1 to MDCKII.

Table 6 summarizes the detailed characterization of compounds **41d** and **41g**. Most of the biological and physicochemical properties of **41d** are superior or equivalent to **41g**. Compound **41d** provided slightly more favorable aqueous solubility and a free fraction ratio of plasma protein binding (aqueous solubility: 94.4 μg/mL; protein binding: 0.4 and 1.9% in human and mouse plasma, respectively) than **41g** (aqueous solubility: 34.1 μg/mL; protein binding: 0.3 and 0.6% in human and mouse plasma, respectively). And the microsomal stabilities of both **41d** and **41g** are comparable. Although **41g** does not suffer from P-gp mediated efflux [Net efflux ratio (NER) = 1.1], **41d** has some issues with the P-gp mediated efflux [NER = 4.3, and the efflux ratio of MDCKII-MDR1 is high (ER = 13.2)]. In mouse pharmacokinetic studies (50 mg/kg, IP), C_{max} and AUC_{inf} values of **41g** are two- and four-times higher than those of **41d**, respectively. This may be due to the difference in the P-gp mediated efflux activity (Table 6; Supporting Information Figure S2). Surprisingly, **41d** was ineffective for tumor growth inhibition in a preliminary mouse xenograft study, despite its superior cellular activity and lower protein binding. (Data not shown) We speculated that P-gp, which is a clinically important transmembrane transporter that confers a multi-drug resistance phenotype to cancer

cells, might contribute to pharmacokinetic profile and drug resistance to result in the lack of *in vivo* efficacy of **41d**.[28] Hence, compound **41g** was chosen as the best candidate for further development.

Table 6. Comparison of the physicochemical/biochemical properties and PK profiles of 41d and 41g.

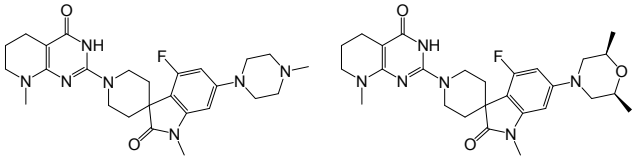

Compound		**41d**	**41g**
Aqueous solubility (pH7.4 in PBS; μg/ml))		94.5	34.1
PAMPA (4 h; x 10^{-6} cm/s)		12.8	12.4
P-gp efflux: NER[a]		4.3	1.1
MDCKII-MDR1		13.2	1.0
MDCKII		3.1	0.9
Liver microsomal stability:	Mouse	54.9 / 30.5	49.7 / 28.7
30min / 60min	Rat	80.2 / 65.3	57.3 / 44.0
(Remaining %)	Human	72.7 / 54.5	73.0 / 55.9
Human/Mouse protein binding: (% free)		Hu: 0.4%, Mo: 1.9%	H: 0.3%, Mo: 0.6%
Mouse IP administration:[b, d]	t_{max} (h)	0.5	1
	C_{max} (μmol/L)	53.6	102
	$t_{1/2}$ (h)	2.5	1.9
	AUC_{inf} (μmol h/L)	207	607
Mouse PO administration:[c, d]	t_{max} (h)	0.25	1
	C_{max} (μmol/L)	21.2	121
	$t_{1/2}$ (h)	4.0	1.8
	AUC_{inf} (μmol h/L)	77	594

[*a*] Net efflux ratio (NER) was calculated as the ratio of the value of MDCKII-MDR1 to MDCKII. [*b*] Intraperitoneal administration of **41d** and **41g** at a dose of 50 mg/kg to male ICR mouse. [*c*] Oral administration of **41d** and **41g** at a dose of 50 mg/kg to male ICR

mouse. [*d*] Pharmacokinetic parameters were calculated using the program, Phoenix WinNolin ver. 8.1.0. [29]

Efforts to minimize P-gp mediated efflux. For optimal pharmacokinetics, we focused on the P-gp mediated efflux potential of our tankyrase inhibitor series. By taking advantage of the available cryo-electron microscopy structure of P-gp/paclitaxel complex,[30] we analyzed the relationship between the structure and the potential for P-gp mediated efflux.

Substitutions at the 1- and 6-positions of the spiroindolinone moiety affect the P-gp efflux ratio and NER (Tables 3−5). Among the 1-substituted spiroindolinone derivatives, the introduction of an oxetanylmethyl (**11f**) or a cyanomethyl (**11d**) group lead to higher NERs. These compounds have a common structural feature. Unlike compounds equipped with other flexible chain substituents from the 1-position of spiroindolinone, both have a rigid hydrogen bond acceptor with an appropriate distance [3.4 (**11f**) and 4.4 Å (**11d**)]. The P-gp efflux data of **11** and **11h** indicated that the introduction of an additional hydroxyl group increases the P-gp efflux ratio of MDCK-MDR1. The three-dimensional cryo-electron microscopy structure of P-gp and paclitaxel suggest that the paclitaxel binding site is mostly hydrophobic, and some hydrogen bond donors/acceptors such as Tyr310, Gln946, and Gln990 can be used to excrete

paclitaxel.[30] A recent report indicated that increasing the hydrogen bond acceptor ability leads to a higher MDR1 efflux activity.[31] Based on our docking study between the paclitaxel binding site and our series of tankyrase inhibitors, the hydrogen bond acceptors of **11f** and **11d** and the hydroxyl group(s) of **11** and **11h** may contribute to the interaction with those residues and enhance P-gp efflux activity.

Among the 6-substituted derivatives such as **37g** and **37h**, the presence of basic amine moieties on the 6-position of spiroindolinone increases NERs. Since the P-gp/paclitaxel binding site is very hydrophobic and has many aromatic amino acids, including Phe and Tyr, compounds with a basic amino group can form cation-π interactions with the aromatic sidechains, increasing the P-gp efflux potentials. These findings are consistent with recent reports that the presence of a positive ionizable amine facilitates the efflux, and that the reduction of pKa of the piperidine moiety reduces the P-gp efflux potentials.[32,33] The introduction of a 2,6-dimethylmorpholine moiety with **41g** lowers the P-gp efflux activity, presumably due to the lack of basicity of the morpholine and the steric congestion of two methyl substituents around the morpholine oxygen. The introduction of a carboxyl group with **11g** and **37j** reduces the

P-gp efflux ratio regardless of the substituted position, which is consistent with the hydrophobic environment without positively charged residues in the P-gp paclitaxel binding site.

Interactions of compound 41g and TNKS2 in the co-crystal structure. Similar to RK-287107 (**1**),[21] crystal structure of TNKS2-**41g** complex (PDB ID: 6KRO, Figure 3 and Supporting Information Table S7) presents the MTPP moiety of **41g** in the nicotinamide binding site. The carbonyl oxygen of the MTPP forms two hydrogen bonds with the hydroxyl group of Ser1068 and the main chain NH group of Gly1032. The nitrogen adjacent to the carbonyl group of the MTPP also forms a hydrogen bond with the main chain carbonyl group of Gly1032. In addition, the MTPP moiety participates in the π-π interaction with Tyr1071. The *N*-methyl group in the MTPP moiety forms a CH-π interaction with Tyr1060. The spiroindolinone moiety, which constitutes the spiro-ring junction, forms the same interactions as the spiroindoline moiety of **1**.[21] The aromatic ring of the indolinone forms T-shaped π-π and CH-π interactions with Phe1035 and Ile1075, respectively. The oxygen of the indolinone amide moiety interacts with the main

chain NH of Tyr1060 via a water molecule. The 2,6-dimethylmorpholine group substituted at the 6-position of indolinone is outside of the enzyme binding site.

Table 7. Comparison of in vitro and rat pharmacokinetic properties of RK-582 (41g), RK-287107 (1) and G007-LK (3).[a]

Compound	**41g** (RK-582)	RK-287107 (**1**)[b]	G007-LK (**4**)[b]
TNKS enz IC_{50} (nM)	36.1	14.3	58.1
TNKS2 enz IC_{50} (nM)	39.2	10.6	85.8
PARP1 enz IC_{50} (nM)	18 187	>100 000	>100 000
PARP2 enz IC_{50} (nM)	1240	2717	>100 000
PARP10 enz IC_{50} (nM)	8053	19 808	>100 000
TCF reporter HEK293 / DLD-1 IC_{50} (nM)	**0.3 / 3.1**	12.1 / 77.6	4.5 / 26.7
COLO-320DM (CellTiter-Glo) GI_{50} (μM)	**0.23**	1.63	1.5
COLO-320DM (MTT) GI_{50} (μM)	**0.035**	0.45[c]	0.43[c]
RKO (MTT) GI_{50} (μM)	>10	>10	8.90
AXIN2 up-regulation @ 0.1 μM[d]	**5.23**	4.42	5.84
Aqueous solubility (pH7.4; μg/mL)	34.1	72.1	1.5
PAMPA (4 h; x 10^{-6} cm/s)	**12.4**	2.0	11.4
Human / Mouse protein binding (% free)	0.3 / 0.6	0.4 / 1.5	2.8 / 3.5
Human / Mouse microsomal stability (% remaining @ 60 min.)	**55.9 / 28.7**	5.9 / 18.3	100 / 95.8
MDCKII-MDR1 / MDCKII efflux ratio	**1.0 / 0.9**	5.3 / 1.8	3.5 / 1.0
Rat IV[e] nC_0 (μmol/L) [f]	**15.26**	9.84	1.54
$T_{1/2}$ (h)	3.61	3.5	3.3
$nAUC_{inf}$ (μmol h/L) [f]	**10.49**	4.42	0.79
CL_{tot} (L/h/kg)	**0.19**	0.54	2.38
Vdssh (L/kg)	1.02	0.59	1.79
Rat PO [g] C_{max} (μmol/L)	**12.67**	2.28	0.23
T_{max} (h)	0.33	0.25	4.0
AUC_{inf} (μmol h/L)	**33.01**	7.92	2.33
F (%)	**~100**	59.8	97.8

[*a*] Bold characters denote improved properties compared to RK-287107. [*b*] Data are from ref. 21. [*c*] Data are from ref. 20. [*d*] Western plot analysis of the compounds was

simultaneously performed. [*e*] Rat intravenous administration at a dose of 3 mg/kg for **41g**, and 1 mg/kg for RK-287107 and G007-LK, male Sprague-Dawley rat. [*f*] nC_0 and $nAUC_{inf}$ were normalized values at a dose of 1 mg/kg for comparison. [*g*] Oral administration at a dose of 3 mg/kg for **41g**, RK-287107 and G007-LK, male Sprague-Dawley rat.

Biological properties. The biological properties of **41g** were evaluated and compared to those of RK-287107 and G007-LK (Table 7). To assess the biological target selectivity of **41g**, inhibitions of human PARP family member enzymes PARP1, PARP2 (poly ADP-ribosylation), and PARP10 (mono ADP-ribosylation) were studied. The enzyme inhibitory activity of **41g** for TNKS (IC_{50}: 39.1 nM) is the same as for TNKS2 (IC_{50}: 36.2 nM), and those activities are comparable with that of RK-287107 and G007-LK. None of the tested PARP enzymes are strongly inhibited by **41g**. The IC_{50} values of **41g** for PARP1, PARP2, and PARP10 are 18 187 nM (504-fold compared to TNKS), 1240 nM (34-fold) and 8053 nM (223-fold), respectively (Supporting Information Figure S3).

The methyl substituent at the 8-position of tetrahydropyridopyrimidinone has a CH-π

interaction with Tyr1060 of TNKS2, increasing the inhibitory activity as mentioned previously. On the other hand, when binding with PARP2, the 8-methyl substituent probably has a CH-π interaction with Tyr462, which interacts with an aromatic ring of Olaparib (Supporting Information Figure S4). Thus, the 8-methyl substituent may contribute to the enhanced inhibitory activities of PARPs, and consequently the slightly lower enzyme selectivity against PARPs.

Compound **41g** exhibits a high potency for the inhibition of TCF reporter activities at IC_{50} values of HEK293 (0.3 nM) and DLD-1 cells (3.1 nM). A comparison of the pIC_{50} value of the TNKS enzyme and the TCF reporter activity of these cells reveals that the functional inhibition of Wnt/β-catenin signaling is well correlated with the enzyme inhibitory activity of the MTPP derivatives. The inhibitory activity of the MTTP-containing derivatives is much stronger as compared with the tetrahydroquinazolinone derivatives,[21] probably due to its higher ability of cell penetration (Supporting Information Figure S5).

The antiproliferative effects of **41g** on CRC cells were investigated by a MTT assay. With COLO-320DM, compound **41g** exhibited potent GI_{50} (0.035 μM), high sensitivity,

and sigmoid dependency achieving complete growth inhibition at 10μM. Meanwhile, **41g** does not inhibit the growth of β-catenin-independent RKO cells (Supporting Information Figure S6).

We compared the western blot analysis data of **41g** and the benchmark compound G007-LK. Both **41g** and G007-LK cause the accumulation of AXIN2 along with decreased levels of active β-catenin, which are direct pharmacodynamics biomarkers of tankyrase inhibition. Consequently, **41g** downregulates Wnt/β-catenin signaling in cultured cells by tankyrase inhibition (Figure 4).

Because tankyrase poly(ADP-ribosyl)ates itself and causes its ubiquitin-dependent proteolysis, tankyrase inhibitors prevent the degradation of tankyrase in itself and induce upregulation of the protein level. Our data indicates that **41g** upregulates the protein level of tankyrase whereas the intensity of tankyrase band is diminished in G007-LK-treated cells (Figure 4). This G007-LK-mediated downregulation of tankyrase protein has been observed several times, but not reproducibly, in our experiments for unknown reason. One speculation is that G007-LK binding to the adenosine pocket of tankyrase PARP domain sometimes alters the conformation of the protein, which

inhibits the antibody recognition of tankyrase during western blot analysis. Actually, we have observed that G007-LK upregulates the tankyrase protein levels in other experimental settings,[20,34] and that both **41g** and G007-LK induced AXIN2 accumulation and downregulation of β-catenin..

Pharmacokinetic profiles. Pharmacokinetic studies of mouse intraperitoneal and oral administration at a dose of 20 mg/kg indicate that the maximum concentration (C_{max}) of **41g** is measured at 76.6 (PO) and 75.6 μmol/L (IP), and that AUC_{inf} is 326 (PO) and 266 μmol h/L (IP) (Figure 5, Table 8). Hence, the pharmacokinetics, including oral absorption, of **41g** in mouse is significantly improved compared to RK-287107.[21] These improvements are attributed to the superior liver microsomal stability and the reduced P-gp mediated efflux activity. Furthermore, pharmacokinetic studies of rat intravenous and oral administration reveal that **41g** is an excellent candidate in the PK parameters and has a remarkable bioavailability (Table 7, Supporting Information Figure S8 and Table S6).

To assess the potential for *in vivo* efficacy, we investigated the inhibition of *in vitro* cytochrome P450 isoforms using a CYP isoform specific substrate-based method. None

of the CYP isoforms are strongly affected by **41g** (EC_{50}: >10 μM) (Supporting Information Table S5).

We then evaluated the antitumor effects of **41g** in a NOD SCID mouse COLO-320DM xenograft model.[20]

Table 8. Pharmacokinetic parameters of the mouse studies.

	Dose (mg)	AUC_{inf} (μmol h/L)	C_{max} (μmol/L)	t_{max} (h)	$t_{1/2}$ (h)
IP[a]	20	266	75.6	1	2.8
PO[a]	20	326	76.6	1	1.7

[*a*] Pharmacokinetic parameters were calculated using the program, Phoenix WinNolin ver. 8.1.0.[29]

Mouse Xenograft model of 41g with COLO-320DM tumor cell. Intraperitoneal administration of **41g** at 10 mg/kg or 20 mg/kg twice daily (20mg/kg or 40 mg/kg daily) with a 5-day on/2-day off a week regimen for 2 weeks yields 68.8% or 71.1% tumor growth inhibition, respectively. Under these conditions, meaningful weight loss or unusual behaviors of the mice are not observed (Figure 6A). Oral administration of **41g**

at 10 mg/kg or 20 mg/kg twice daily with a 5-day on/2-day off regimen for 2 weeks results in 52.3% or 52.0% tumor growth inhibition, respectively (Figure 7A).

To determine the pharmacodynamics of **41g** at the protein level, we performed western blot analysis of the tumor tissues. The AXIN2 levels are elevated in the cytoplasmic extracts from the tumor tissues for both the intraperitoneally and orally administered groups (Figure 6B, 7B). Interestingly, dose-dependent tumor volumes reductions are not observed. The active β-catenin and total β-catenin levels are reduced in the nuclear extracts from the tumor tissues after oral administration, but not from those after intraperitoneal administration (Figure 6B, 7B and Supporting Information Figure S7).

To determine pharmacokinetics of **41g** under the xenograft study, plasma concentrations at the 4 h time point on the 12th day were observed. The dose-dependent concentration levels (PO, twice daily, 10 mg/kg: C_{4h} = 10.1 μmol/L; 20 mg/kg: C_{4h} = 23.3 μmol/L) and little alternation in the drug concentration between the repeated xenograft study (see data above) and the pharmacokinetic study (PO, 20 mg/kg: C_{4h} = 26.9 μmol/L; Figure S8) are validated.

Regarding the intestinal toxicity of **41g**, weight loss, decreased appetite and unusual behaviors of the mice were noticed and moderate levels of epithelial degeneration and reduction of crypt proliferation were observed at an intraperitoneal dosage of 50 mg/kg twice daily in our preliminary experiment (data not shown).

On the other hand, RK-287107 exhibits significant tumor growth inhibition of 47.2% and 51.9% with intraperitoneal (150 mg/kg, bid) and oral administration (300 mg/kg, bid), respectively, as shown in our previous report.[20] Compound **41g** has a statistically significant comparable tumor growth inhibition at 68.8% and 52.3% with intraperitoneal (10 mg/kg, bid) and oral administration (10 mg/kg, bid), respectively.

■ CONCLUSION

Multifactorial optimization of spiroindoline derivative **1** led to the identification of a spiroindolinone compound RK-582 (**41g**). RK-582 is a potent TNKS/TNKS2 inhibitor with an excellent selectivity against other PARP family enzymes, including PARP1 (IC_{50}: 18 187 nM), PARP2 (IC_{50}: 1240 nM) and PARP10 (IC_{50}: 8053 nM). TCF reporter assays in HEK293 and DLD-1 cells (IC_{50}: 0.3 nM and 3.1 nM, respectively), reveal that RK-582 inhibits the Wnt/β-catenin signaling pathway at the cellular level and the proliferation.

RK-582 also inhibits the cell proliferation of human CRC COLO-320DM cells (GI_{50}: 0.23 μM). Western blot analysis in COLO-320DM cells demonstrates that RK-582 modulates the β-catenin pathway by elevating the levels of AXIN2 and reducing the levels of active β-catenin. Supported by its excellent rodent pharmacokinetic profiles, RK-582 exhibits the statistically significant tumor growth inhibition in a COLO-320DM xenograft model when administered intraperitoneally or orally at a dosage of 10 or 20 mg/kg twice daily, respectively. Although weight loss and general toxicity are not observed at doses of 10 or 20 mg/kg twice daily, moderate level of intestinal epithelium disruption occur at a high dosage of 50 mg/kg twice daily, which may be due to the mechanistic toxicity of tankyrase inhibition as suggested by other groups.[23,24] This intestinal toxicity would be unavoidable at higher dose. However, given the excellent tankyrase inhibitory activity and pharmacokinetic profiles, RK-582 would be an effective tool to validate the potential and utility as cancer therapeutic agent. As multiple factors and mechanisms are involved in the onset and progression of cancers, a combination of anti-cancer agents with different mechanisms may offer effective cancer treatments. Systematic co-

administration efficacy studies involving a tankyrase inhibitor such as RK-582 and other anticancer agents in different mechanisms are awaited.[35-39]

■ EXPERIMENTAL SECTION

General Methods. All chemicals were purchased from commercial suppliers TCI, Wako, and Sigma-Aldrich, and used as received unless otherwise specified. NMR spectra were recorded at either 270 MHz (JEOL JNM-Ex270), 400 MHz (JEOL ECS-400 or Bruker 400MHz Advance III HD) spectrometers. Chemical shifts are reported in ppm (δ) referenced to TMS (δ = 0.00 ppm), DMSO (2.50 ppm), and chloroform (7.26 ppm). Temperatures are expressed in degrees Celsius (°C) and are uncorrected. Purity and characterization of all final compounds were established by a combination of LC-MS and NMR analytical techniques. Final compounds were found to be >95% pure by HPLC analysis (λ = 254 nm). LC-MS analysis was performed on a Waters Acquity UPLC analytical system with DAD coupled to a single quadrupole mass spectrometer (ESI-SQ) equipped with an ACQUITY UPLC BEH C18 column, 2.1 mm × 50 mm, 1.7 μm. Method: ESI+, flux of 0.6 mL/min, 5−95% CH_3CN in H_2O + 0.1% TFA, total run time of 2 min. High-resolution mass spectrometry (HRMS) analysis was performed using

hybrid quadrupole/time-of-flight tandem mass spectrometer, Synapt G2 instrument (Waters) for final compounds. Microwave reaction was carried using Initiator 2.5, Biotage Japan.

Materials. **G007-LK** was synthesized by a partially modified method reported in the literature[17].

General Procedure A. To a solution of spiroindoline-3,4'-piperidine or spiroindolinone-3,4'-piperidine derivative (1 equiv., 0.1 mmol) in ethanol (1 ml) were added 2-chloropyrimidin-4(3*H*)-one derivative (1.2 equiv., 0.12 mmol) and triethylamine (1 equiv., 17 μL, 0.12 mmol) at ambient temperature. After stirring at 150 °C for 0.5 h with microwave irradiation, the reaction mixture was quenched with saturated sodium bicarbonate and extracted with chloroform. The organic layer was dried over magnesium sulfate, filtered and evaporated under reduced pressure. The residue was column chromatographed on silica gel (methanol/chloroform = 10:90) to provide the desired product or used for next transformation.

General Procedure B. Cbz-protected compound (1 equiv, 0.94 mmol) was dissolved in methanol (2.5 mL) and 10% Pd-C (50% wet; 0.1 equiv, 0.094 mmol) was added. After

stirring under a hydrogen atmosphere at ambient temperature for 1 h, the mixture was filtered through a Celite pad and washed with methanol. The filtrate was evaporated under reduced pressure to provide the desired product.

2-(4,6-difluoro-1-(2-hydroxyethyl)spiro[indoline-3,4'-piperidin]-1'-yl)-8-methylquinazolin-4(3H)-one (8). The title compound was synthesized according to general procedure A from 2-chloro-8-methylquinazolin-4(3*H*)-one (**17**)[25] and **20**[21] as a white solid (18.6 mg, 44%); LC-MS (ESI): m/z 427 ($M + H^+$). Retention time: 1.36 min. LC Purity: 99%. HRMS m/z ($M + H^+$) calculated for $C_{23}H_{24}F_2N_4O_2 + H^+$: 427.1946 found: 427.1943. ^{1}H NMR (400 MHz, $CDCl_3$) δ [ppm] 1.56-1.92 (m, 2H), 2.32-2.41 (m, 2H), 2.48 (s, 3H), 3.05-3.14 (m, 2H), 3.30-3.34 (m, 2H), 3.59 (s, 2H), 3.84-3.88 (m, 2H), 4.52-4.59 (m, 2H), 6.02-6.10 (m, 2H), 7.03-7.07 (m, 1H), 7.45-7.49 (m, 1H), 7.89-7.92 (m, 1H), 11.21 (br s, 1H).

2-(4,6-difluoro-1-(2-hydroxyethyl)-2-oxospiro[indoline-3,4'-piperidin]-1'-yl)-8-methylquinazolin-4(3H)-one (9). The title compound was synthesized according to general procedure A from **17**[25] and **21**[21] as a white solid (21.0 mg, 48%); LC-MS (ESI): m/z 441 ($M + H^+$). Retention time: 1.28 min. LC Purity: 99%. HRMS m/z ($M + H^+$) calculated for $C_{23}H_{22}F_2N_4O_3 + H^+$: 441.1738, found: 441.1736. ^{1}H NMR (400 MHz,

DMSO-d_6) δ [ppm] 1.82-1.90 (m, 2H), 2.09-2.18 (m, 2H), 2.40 (s, 3H), 3.58-3.64 (m, 2H), 3.73-3.86 (m, 4H), 4.21-4.28 (m, 2H), 4.85 (t, J=5.8 Hz, 1H), 6.80-6.87 (m, 1H), 7.00 (dd, J=9.3, 2.2 Hz, 1H), 7.03-7.08 (m, 1H), 7.48-7.51 (m, 1H), 7.77-7.81 (m, 1H), 11.45 (br s, 1H).

2-(4,6-difluoro-1-(2-hydroxyethyl)spiro[indoline-3,4'-piperidin]-1'-yl)-8-methyl-5,6,7,8-tetrahydropyrido[2,3-d]pyrimidin-4(3H)-one (10). Compound **22** was synthesized according to general procedure A form 2-chloropyrido[2,3-*d*]pyrimidin-4(3*H*)-one (**18**)[26] and **20**[21].

Compound **22** was dissolved in DMF (1 mL) and iodomethane (3 equiv, 19 µL, 0.3 mmol) was added at ambient temperature. After stirring at 100 °C for 3 h, the solvent was evaporated under reduced pressure. The residue was dissolved in ethanol (1 mL) and platinum (IV) oxide (0.1 equiv, 2.3 mg, 0.01 mmol) was added. After stirring under a hydrogen atmosphere at ambient temperature for 14 h, the mixture was filtered through a Celite pad and washed with ethanol. The filtrate was evaporated under reduced pressure. The residue was column chromatographed on silica gel (methanol/chloroform = 10:90) to give 23.7 mg (55%, 0.055 mmol) of **10** as a white solid; LC-MS (ESI): m/z

432 ($M + H^+$). Retention time: 1.34 min. LC Purity: 98%. HRMS m/z ($M + H^+$) calculated for $C_{22}H_{27}F_2N_5O_2 + H^+$: 432.2211, found: 432.2209. ^1H NMR (400 MHz, DMSO-d_6) δ [ppm] 1.65-1.78 (m, 4H), 1.87-1.97 (m, 2H), 2.27-2.32 (m, 2H), 2.82-2.91 (m, 2H), 2.98 (s, 3H), 3.19-3.24 (m, 4H), 3.56-3.61 (m, 4H), 4.27-4.34 (m, 2H), 4.71 (t, J=5.4 Hz, 1H), 6.10-6.19 (m, 2H), 10.31 (br s, 1H).

1-(2-hydroxyethyl)-2-oxospiro[indoline-3,4'-piperidin]-1'-yl)-8-methyl-5,6,7,8-tetrahydropyrido[2,3-d]pyrimidin-4(3H)-one (11). The title compound was prepared following the same procedure of **10** from **18**[26] and **21**[21] as a white solid (16.8 mg, 38%); LC-MS (ESI): m/z 446 ($M + H^+$). Retention time: 1.24min. LC Purity: 97%. HRMS m/z ($M + H^+$) calculated for $C_{22}H_{25}F_2N_5O_3 + H^+$: 446.2004, found: 446.1998. ^1H NMR (400 MHz, $CDCl_3$) δ [ppm] 1.79-1.88 (m, 4H), 2.20-2.29 (m, 2H), 2.42-2.47 (m, 2H), 3.07 (s, 3H), 3.23-3.28 (m, 2H), 3.82-3.91 (m, 6H), 4.16-4.23 (m, 2H), 6.42-6.48 (m, 1H), 6.55 (dd, J=8.5, 2.0 Hz, 1H).

4,6-difluoro-1-methyl-1'-(8-methyl-4-oxo-3,4,5,6,7,8-hexahydropyrido[2,3-d]pyrimidin-2-yl)spiro[indoline-3,4'-piperidin]-2-one (11a).

11a.1. To a solution of **24** (1 equiv, 529 mg, 1.42 mmol) in DMF (7 mL) was added iodomethane (1.5 equiv, 133 μL, 2.13 mmol) and sodium hydride (60% dispersion in paraffin liquid; 1.5 equiv, 85.2 mg, 2.13 mmol) at ambient temperature. After stirring for

1 h, saturated ammonium chloride was added, and the mixture was extracted with ethyl acetate and washed with brine. The organic layer was dried over magnesium sulfate, filtered and evaporated under reduced pressure. The residue was column chromatographed on silica gel (ethyl acetate/n-hexane = 35:65) to give 363 mg (66%, 0.94 mmol) of benzyl 4,6-difluoro-1-methyl-2-oxospiro[indoline-3,4'-piperidine]-1'-carboxylate (**25a**).

11a. 2. Compound **25a** (1 equiv, 363 mg, 0.94 mmol) was treated by general procedure B to give 180 mg (76%, 0.71 mmol) of 4,6-difluoro-1-methylspiro[indoline-3,4'-piperidin]-2-one (**21a**), and then treated by general procedure A with **18** to give 39.7 mg (quant., 0.1 mmol) of **26a**.

11a. 3. To a solution of **26a** (1 equiv, 39.7 mg, 0.1 mmol) in DMF (0.5 mL) was added iodomethane (3 equiv, 19 μL, 0.3 mmol) at ambient temperature. After stirring at 100 °C for 3 h, the solvent was evaporated. The residue was dissolved in ethanol (1 mL) and platinum (IV) oxide (0.1 equiv, 2.3 mg, 0.01 mmol) was added. After stirring under a hydrogen atmosphere at ambient temperature for 14 h, the mixture was filtered through a Celite pad and washed with methanol. The filtrate was evaporated under reduced

pressure and the residue was column chromatographed on silica gel (methanol/chloroform = 10:90) to give 26.2 mg (63%, 0.063 mmol) of **11a** as a white powder; LC-MS (ESI): m/z 416 ($M + H^+$). Retention time: 1.37 min. LC Purity: 98%. HRMS m/z ($M + H^+$) calculated for $C_{21}H_{23}F_2N_5O_2 + H^+$: 416.1898, found: 416.1894. ^1H NMR (400 MHz, $CDCl_3$) δ [ppm] 1.78-1.87 (m, 4H), 2.19-2.28 (m, 2H), 2.43-2.48 (m, 2H), 3.07 (s, 3H), 3.18 (s, 3H), 3.23-3.27 (m, 2H), 3.86-3.94 (m, 2H), 4.21-4.27 (m, 2H), 6.42 (dd, J=8.3, 2.1 Hz, 1H), 6.45-6.51 (m, 1H), 10.82 (br s, 1H).

2-(4,6-difluoro-1-(2-methoxyethyl)-2-oxospiro[indoline-3,4'-piperidin]-1'-yl)-8-methyl-5,6,7,8-tetrahydropyrido[2,3-d]pyrimidin-4(3H)-one (11b). To a solution of **24** (1 equiv, 37.2 mg, 0.1 mmol) in DMF (1 mL) were added 2-bromoethyl methyl ether (1.5 equiv, 14 μL, 0.15 mmol) and potassium carbonate (3 equiv, 41.5 mg, 0.3 mmol) at ambient temperature. After stirring at 80 °C for 1 h, saturated ammonium chloride was added. The mixture was extracted with ethyl acetate and washed with brine. The organic layer was dried over magnesium sulfate, filtered and evaporated under reduced pressure. The residue was column chromatographed on silica gel (ethyl acetate/n-hexane =

35:65) to give 43.0 mg (quant., 0.1 mmol) of benzyl 4,6-difluoro-1-(2-methoxyethyl)-2-oxospiro[indoline-3,4'-piperidine]-1'-carboxylate (**25b**).

Compound **25b** (1 equiv, 363 mg, 0.94 mmol) was treated by general procedure B to give crude 4,6-difluoro-1-(2-methoxyethyl)spiro[indoline-3,4'-piperidin]-2-one (**21b**), and then treated by general procedure A with 2-chloro-8-methyl-5,6,7,8-tetrahydropyrido[2,3-*d*]pyrimidin -4(3H)-one (**28**) to give 45.2 mg (98%, 0.098 mmol) of **11b** as a white powder; LC-MS (ESI): m/z 460 ($M + H^+$). Retention time: 1.39 min. LC Purity: 97%. HRMS m/z ($M + H^+$) calculated for $C_{23}H_{27}F_2N_5O_3 + H^+$: 460.2160, found: 460.2151. ^{1}H NMR (400 MHz, $CDCl_3$) δ [ppm] 1.77-1.87 (m, 4H), 2.21-2.30 (m, 2H), 2.43-2.48 (m, 2H), 3.07 (s, 3H), 3.23-3.27 (m, 2H), 3.33 (s, 3H), 3.58-3.62 (m, 2H), 3.82-3.93 (m, 4H), 4.22-4.30 (m, 2H), 6.42-6.49 (m, 1H), 6.58 (dd, J=8.7, 2.1Hz, 1H), 10.83 (br s, 1H).

4,6-difluoro-1'-(8-methyl-4-oxo-3,4,5,6,7,8-hexahydropyrido[2,3-d]pyrimidin-2-yl)-1-(2,2,2-trifluoroethyl)spiro[indoline-3,4'-piperidin]-2-one (11c). The title compound was synthesized following the same procedure of **11b** as a white solid (30.0 mg, 62%); LC-MS (ESI): m/z 484 ($M + H^+$). Retention time: 1.46 min. LC Purity: 98%. HRMS m/z (M +

H^+) calculated for $C_{22}H_{22}F_5N_5O_2$ + H^+: 484.1772, found: 484.1771. ^{1}H NMR (400 MHz, $CDCl_3$) δ [ppm] 1.78-1.86 (m, 4H), 2.26-2.35 (m, 2H), 2.42-2.48 (m, 2H), 3.07 (s, 3H), 3.23-3.27 (m, 2H), 3.78-3.87 (m, 2H), 4.24-4.36 (m, 4H), 6.51-6.58 (m, 2H), 11.00 (br s, 1H).

2-(4,6-difluoro-1'-(8-methyl-4-oxo-3,4,5,6,7,8-hexahydropyrido[2,3-d]pyrimidin-2-yl)-2-oxospiro[indoline-3,4'-piperidin]-1-yl)acetonitrile (11d). The title compound was synthesized following the same procedure of **11b** as a white solid (18.3 mg, 42%); LC-MS (ESI): m/z 441 (M + H^+). Retention time: 1.34 min. LC Purity: 97%. HRMS m/z (M + H^+) calculated for $C_{22}H_{22}F_2N_6O_2$ + H^+: 441.1851, found: 441.1849. ^{1}H NMR (400 MHz, $CDCl_3$) δ [ppm] 1.80-1.87 (m, 4H), 2.26-2.34 (m, 2H), 2.43-2.47 (m, 2H), 3.07 (s, 3H), 3.23-3.27 (m, 2H), 3.76-3.85 (m, 2H), 4.30-4.37 (m, 2H), 4.63 (s, 2H), 6.56-6.62 (m, 2H), 11.11 (br s, 1H).

4,6-difluoro-1'-(8-methyl-4-oxo-3,4,5,6,7,8-hexahydropyrido[2,3-d]pyrimidin-2-yl)-1-((methylsulfonyl)methyl)spiro[indoline-3,4'-piperidin]-2-one (11e). The title compound was synthesized following the same procedure of **11b** as a white solid (23.1 mg, 45%); LC-MS (ESI): m/z 494 (M + H^+). Retention time: 1.28 min. LC Purity: >99%. HRMS m/z

(M + H^+) calculated for $C_{22}H_{25}F_2N_5O_4S$ + H^+: 494.1674, found: 494.1668. ^1H NMR (400 MHz, $CDCl_3$) δ [ppm] 1.79-1.88 (m, 4H), 2.29-2.39 (m, 2H), 2.42-2.47 (m, 2H), 2.97 (s, 3H), 3.07 (s, 3H), 3.23-3.28 (m, 2H), 3.75-3.84 (m, 2H), 4.32-4.39 (m, 2H), 4.91 (s, 2H), 6.54-6.61 (m, 1H), 6.75 (dd, J=8.2, 1.8 Hz, 1H), 11.18 (br s, 1H).

2-(4,6-difluoro-1-(oxetan-3-ylmethyl)-2-oxospiro[indoline-3,4'-piperidin]-1'-yl)-8-methyl-5,6,7,8-tetrahydropyrido[2,3-d]pyrimidin-4(3H)-one (11f). To a solution of **24** (1 equiv, 52.9 mg, 0.142 mmol) in THF (1 mL) were added 3-oxetane-1-methanol (3 equiv, 37.6 mg, 0.427 mmol), ca. 2.2M diethyl azodicarboxylate in toluene (3 equiv, 194 μL, 0.427 mmol) and triphenylphosphine (3 equiv, 112 mg, 0.427 mmol) at ambient temperature. After stirring for 1 h, the solvent was evaporated under reduced pressure. The residue was column chromatographed on silica gel (ethyl acetate/n-hexane = 50:50) to give 51.8 mg (82%, 0.117 mmol) of benzyl 4,6-difluoro-1-(oxetan-3-ylmethyl)-2-oxospiro[indoline-3,4'-piperidine]-1'-carboxylate (**25f**).

Compound **25f** (1 equiv, 51.8 mg, 0.12 mmol) was treated by general procedure B to give crude 4,6-difluoro-1-(oxetan-3-ylmethyl)spiro[indoline-3,4'-piperidin]-2-one (**21f**), and then treated by general procedure A with **28** to give 22.6 mg (41%, 0.048 mmol) of

11f as a white solid; LC-MS (ESI): m/z 472 (M + H^+). Retention time: 1.32 min. LC Purity: 99%. HRMS m/z (M + H^+) calculated for $C_{24}H_{27}F_2N_5O_3$ + H^+: 472.2160, found: 472.2152. ^{1}H NMR (400 MHz, $CDCl_3$) δ [ppm] 1.74-1.86 (m, 4H), 2.20-2.30 (m, 2H), 2.42-2.47 (m, 2H), 3.06 (s, 3H), 3.22-3.27 (m, 2H), 3.35-3.47 (m, 1H), 3.82-3.92 (m, 2H), 3.98 (d, J=7.1 Hz, 2H), 4.24-4.32 (m, 2H), 4.50-4.55 (m, 2H), 4.78 (dd, J=7.7, 6.4 Hz, 2H), 6.42 (dd, J=8.4, 2.0 Hz, 1H), 6.45-6.51 (m, 1H), 11.11 (br s, 1H).

2-(4,6-difluoro-1'-(8-methyl-4-oxo-3,4,5,6,7,8-hexahydropyrido[2,3-d]pyrimidin-2-yl)-2-oxospiro[indoline-3,4'-piperidin]-1-yl)acetic acid (11g). Methyl 2-(4,6-difluoro-1'-(8-methyl-4-oxo-3,4,5,6,7,8-hexahydropyrido[2,3-*d*]pyrimidin-2-yl)-2-oxospiro[indoline-3,4'-piperidin]-1-yl)acetate (**11g-Me**) was synthesized from the corresponding intermediate (**21g**) and **28** following the same procedure of **11b**.

Compound **11g-Me** (1 equiv, 28.9 mg, 0.061 mmol) was dissolved in ethanol (1 mL) and added 1N aq. sodium hydroxide (2.2 equiv, 130 µL, 0.130 mmol). After stirring for 2 h, the reaction mixture was quenched with 1N aq. hydrochloric acid and extracted with chloroform. The organic layer was dried over magnesium sulfate, filtered and evaporated under reduced pressure. The residue was column chromatographed on

silica gel (methanol/chloroform = 50:50) to give 15.0 mg (54%, 0.033 mmol) of **11g** as a white solid; LC-MS (ESI): m/z 460 ($M + H^+$). Retention time: 1.26 min. LC Purity: >99%. HRMS m/z ($M + H^+$) calculated for $C_{22}H_{23}F_2N_5O_4 + H^+$: 460.1796, found: 460.1793. ^1H NMR (400 MHz, $CDCl_3$) δ [ppm] 1.40-1.79 (m, 4H), 1.82-1.91 (m, 2H), 2.44-2.56 (m, 2H), 3.09 (s, 3H), 3.26-3.37 (m, 2H), 3.69-3.99 (m, 4H), 3.36-3.90 (m, 2H), 6.31-6.38 (m, 1H), 6.39-6.51 (m, 1H), 11.94 (br s, 1H).

1-(2,3-dihydroxypropyl)-4,6-difluoro-1'-(8-methyl-4-oxo-3,4,5,6,7,8-hexahydropyrido[2,3-d]pyrimidin-2-yl)spiro[indoline-3,4'-piperidin]-2-one (11h). To a solution of **24** (1 equiv, 149 mg, 0.40 mmol) in DMF (2 mL) was added *tert*-butyldimethyl(oxiran-2-ylmethoxy) silane (1.5 equiv, 113 mg, 0.60 mmol) and sodium hydride (60% dispersion in paraffin liquid; 1.2 equiv, 19.2 mg, 0.48 mmol) at ambient temperature. After stirring at 100 °C for 5 h, saturated ammonium chloride was added, and the mixture was extracted with ethyl acetate. The organic layer was washed with brine, dried over magnesium sulfate, filtered and evaporated under reduced pressure. The residue was column chromatographed on silica gel (ethyl acetate/n-hexane = 20:80) to give 44 mg (25%,

0.10 mmol) of benzyl 1-(2,3-dihydroxypropyl)-4,6-difluoro-2-oxospiro[indoline-3,4'-piperidine]-1'-carboxylate (**25h**).

Compound **25h** (1 equiv, 27 mg, 0.06 mmol) was treated by general procedure B to give crude 1-(2,3-dihydroxypropyl)-4,6-difluorospiro[indoline-3,4'-piperidin]-2-one (**21h**), and then treated by general procedure A with **28** to give 23 mg (81%, 0.048 mmol) of **11h** as a white solid; LC-MS (ESI): m/z 476 ($M + H^+$). Retention time: 1.20 min. LC Purity: >99%. HRMS m/z ($M + H^+$) calculated for $C_{23}H_{27}F_2N_5O_4 + H^+$: 476.2109, found: 476.2108. ^{1}H NMR (400 MHz, $CDCl_3$) δ [ppm] 1.73-1.89 (m, 4H), 2.12-2.34 (m, 2H), 2.35-2.48 (m, 2H), 3.07 (s, 3H), 3.26 (t, J=5.56 Hz, 2H), 3.53-3.62 (m, 1H), 3.64-3.77 (m,2H), 3.77-4.02 (m, 4H), 4.10-4.22 (m, 2H), 6.40-6.50 (m, 1H), 6.57-6.65 (m, 1H).

2-(4,6-difluoro-1-(2-hydroxyethyl)spiro[indoline-3,4'-piperidin]-1'-yl)-7-methyl-3H-pyrrolo[2,3-d]pyrimidin-4(7H)-one (12). The title compound was synthesized according to general procedure A from 2-chloro-7-methyl-3,7-dihydro-4*H*-pyrrolo[2,3-*d*]pyrimidin-4-one (**19**)[27] and **20**[21] as a white solid (22.3 mg, 54%); LC-MS (ESI): m/z 416 ($M + H^+$). Retention time: 1.35 min. LC Purity: >99%. HRMS m/z ($M + H^+$) calculated for $C_{21}H_{23}F_2N_5O_2 + H^+$: 416.1898, found: 416.1898. ^{1}H NMR (400 MHz, DMSO-d_6): δ [ppm]

1.71-1.77 (m, 2H), 1.97-2.06 (m, 2H), 2.91-3.00 (m, 2H), 3.21-3.25 (m, 2H), 3.56 (s, 3H), 3.58-3.63 (m, 4H), 4.27-4.34 (m, 2H), 4.73 (t, J=5.5 Hz, 1H), 6.11-6.21 (m, 2H), 6.25 (d, J=3.3 Hz, 1H), 6.77 (d, J=3.3 Hz, 1H), 10.77 (br s, 1H).

2-(4,6-difluoro-1-(2-hydroxyethyl)-2-oxospiro[indoline-3,4'-piperidin]-1'-yl)-7-methyl-3H-pyrrolo[2,3-d]pyrimidin-4(7H)-one (13). The title compound was synthesized according to general procedure A from **19**[27] and **21**[21] as a white solid (7.9 mg, 18%); LC-MS (ESI): m/z 430 ($M + H^+$). Retention time: 1.26 min. LC Purity: 95%. HRMS m/z ($M + H^+$) calculated for $C_{21}H_{21}F_2N_5O_3 + H^+$: 430.1691, found: 430.1690. ^1H NMR (400 MHz, $CDCl_3$) δ [ppm] 1.86-1.92 (m, 2H), 2.27-2.36 (m, 2H), 3.61 (s, 3H), 3.83-4.00 (m, 6H), 4.18-4.25 (m, 2H), 4.41-4.47 (m, 2H), 6.52-6.57 (m, 2H), 10.05 (br s, 1H)

4,6-difluoro-1-(2-hydroxyethyl)-1'-(7-methyl-4-oxo-4,5,6,7-tetrahydro-3H-pyrrolo[2,3-d]pyrimidin-2-yl)spiro[indoline-3,4'-piperidin]-2-one (14). To a solution of **12** (1 equiv, 33.4 mg, 0.08 mmol) in methanol (5 mL) were added 10% Pd-C (50% wet; 0.2 equiv, 34.2 mg, 0.016 mmol) and acetic acid (0.5 mL). After stirring under a hydrogen atmosphere at ambient temperature for 17 h, the mixture was filtered through a Celite pad and washed with methanol. The filtrate was evaporated under reduced pressure,

and the residue was purified by preparative layer chromatography (chloroform/methanol = 95:5) to give 9.3 mg (28%, 0.022 mmol) of **14** as a white powder; LC-MS (ESI): m/z 418 ($M + H^+$). Retention time: 1.09 min. LC Purity: >99%. HRMS m/z ($M + H^+$) calculated for $C_{21}H_{25}F_2N_5O_2 + H^+$: 417.1976, found: 417.1980. ^1H NMR (270 MHz, $CDCl_3$), δ: 1.74-1.86 (m, 4H), 2.79 (t, J=8.9 Hz, 2H), 2.88 (s, 3H), 2.92-3.16 (m, 3H), 3.29 (t, J=5.3 Hz, 2H), 3.40-3.49 (m, 2H), 3.54 (s, 2H), 3.83 (t, J=5.3 Hz, 2H), 4.33-4.46 (m, 2H), 5.98-6.10 (m, 2H).

4,6-difluoro-1-(2-hydroxyethyl)-1'-(7-methyl-4-oxo-4,5,6,7-tetrahydro-3H-pyrrolo[2,3-d]pyrimidin-2-yl)spiro[indoline-3,4'-piperidin]-2-one (15). Title compound was synthesized from **13** following the same procedure of **14** as a white powder (24.4 mg, 64%); LC-MS (ESI): m/z 432 ($M + H^+$). Retention time: 1.10 min. LC Purity: 95%. HRMS m/z ($M + H^+$) calculated for $C_{20}H_{26}N_4O_2 + H^+$: 432.1847, found: 432.1843. ^1H NMR (400 MHz, $CDCl_3$) δ [ppm] 1.85-1.91 (m, 2H), 2.17-2.26 (m, 2H), 2.66-2.72 (m, 2H), 2.87 (s, 3H), 3.41-3.47 (m, 2H), 3.79-3.92 (m, 6H), 4.28-4.35 (m, 2H), 6.34-6.41 (m, 1H), 6.56 (dd, J=8.7, 2.0 Hz, 1H), 10.11 (br s, 1H).

4-fluoro-6-methoxy-1-methyl-1'-(8-methyl-4-oxo-3,4,5,6,7,8-hexahydropyrido[2,3-d]pyrimidin-2-yl)spiro[indoline-3,4'-piperidin]-2-one (37a). To a solution of **33** (1 equiv, 36.4 mg, 0.1 mmol) in chloroform (1 mL) was added trifluoroacetic acid (130 equiv, 1 mL, 13 mmol) at ambient temperature. After stirring for 1 h, the mixture was quenched with saturated sodium bicarbonate and extracted with chloroform. The organic layer was dried over magnesium sulfate, filtered and evaporated under reduced pressure (**36a**).

The residue (**36a**) was treated by general procedure A with **28** to give 31.4 mg (74%, 0.073 mmol) of **37a** as a white powder; LC-MS (ESI): m/z 362 ($M + H^+$). Retention time: 1.35 min. LC Purity: 99%. HRMS m/z ($M + H^+$) calculated for $C_{22}H_{26}FN_5O_3 + H^+$: 428.2098, found: 428.2096. ^1H NMR (400 MHz, $CDCl_3$) δ [ppm] 1.79-1.87 (m, 4H), 2.15-2.24 (m, 2H), 2.44-2.49 (m, 2H), 3.07 (s, 3H), 3.17 (s, 3H), 3.23-3.27 (m, 2H), 3.81 (s, 3H), 3.89-3.97 (m, 2H), 4.14-4.21 (m, 2H), 6.23-6.28 (m, 2H), 10.45 (br s, 1H).

4-fluoro-6-(2-hydroxyethoxy)-1-methyl-1'-(8-methyl-4-oxo-3,4,5,6,7,8-hexahydropyrido[2,3-d]pyrimidin-2-yl)spiro[indoline-3,4'-piperidin]-2-one (37b). *tert*-Butyl 4-fluoro-6-methoxy-1-methyl-2-oxospiro[indoline-3,4'-piperidine]-1'-carboxylate (**33**; 1 equiv, 27.7 mg, 0.076 mmol) was dissolved in chloroform (1 mL) and 17% boron

tribromide in dichloromethane (20 equiv, 1.5 mL, 1.5 mmol) was added at 0 °C. After stirring at ambient temperature for 14 h, the reaction mixture was quenched with methanol (1 mL), neutralized with 5N aq. sodium hydroxide and di-*tert*-butyl dicarbonate (1.5 equiv, 26 μL, 0.114 mmol) was added. After stirring at ambient temperature for 1 h, the reaction mixture was quenched with 1N aqueous hydrochloric acid and extracted with chloroform. The organic layer was dried over magnesium sulfate, filtered and evaporated under reduced pressure. The residue was column chromatographed on silica gel (ethyl acetate/n-hexane = 50:50) to give 26.6 mg (quant., 0.076 mmol) of *tert*-butyl 4-fluoro-6-hydroxy-1-methyl-2-oxospiro [indoline-3,4'-piperidine]-1'-carboxylate (**34**).

To a solution of **34** (1 equiv, 70.1 mg, 0.2 mmol) in DMF (1 mL) was added 2-iodoehanol (1.5 equiv, 23 μL, 0.3 mmol) and potassium carbonate (3 equiv, 82.9 mg, 0.6 mmol) at ambient temperature. After stirring at 80 °C for 3 h, the mixture was diluted with water, extracted with ethyl acetate and washed with brine. The organic layer was dried over magnesium sulfate, filtered and evaporated under reduced pressure. The residue was dissolved in chloroform (1 mL) and added trifluoroacetic acid (65 equiv, 1

mL, 13 mmol) at ambient temperature. After stirring for 1 h, the mixture was quenched with saturated sodium bicarbonate and extracted with chloroform. The organic layer was dried over magnesium sulfate, filtered and evaporated under reduced pressure. The residue was treated by general procedure A with **28** to give 24.4 mg (27%, 0.053 mmol) of **37b** as a white powder; LC-MS (ESI): m/z 458 ($M + H^+$). Retention time: 1.19 min. LC Purity: 97%. HRMS m/z ($M + H^+$) calculated for $C_{20}H_{21}FN_4O_2 + H^+$: 458.2204, found: 458.2199. ^{1}H NMR (400 MHz, DMSO-d_6) δ [ppm] 1.71-1.80 (m, 4H), 1.92-2.01 (m, 2H), 2.29-2.34 (m, 2H), 3.07 (s, 3H), 3.12 (s, 3H), 3.20-3.25 (m, 2H), 3.69-3.79 (m, 4H), 4.01-4.11 (m, 4H), 4.88 (t, J=5.4 Hz, 1H), 6.46 (dd, J=12.2, 2.0 Hz, 1H), 6.56 (d, J=2.0 Hz, 1H), 10.35 (br s, 1H).

4-fluoro-6-(2-methoxyethoxy)-1-methyl-1'-(8-methyl-4-oxo-3,4,5,6,7,8-hexahydropyrido[2,3-d]pyrimidin-2-yl)spiro[indoline-3,4'-piperidin]-2-one (37c) The title compound was synthesized following the same procedure of **37d** as a white solid (24.2 mg, 51%); LC-MS (ESI): m/z 472 ($M + H^+$). Retention time: 1.33 min. LC Purity: 98%. HRMS m/z ($M + H^+$) calculated for $C_{24}H_{30}FN_5O_4 + H^+$: 472.2360, found: 472.2360. ^{1}H NMR (400 MHz, $CDCl_3$) δ [ppm] 1.79-1.87 (m, 4 H), 2.14-2.23 (m, 2 H), 2.44-2.49 (m, 2

H), 3.08 (s, 3 H), 3.15 (s, 3 H), 3.25-3.29 (m, 2 H), 3.45 (s, 3 H), 3.73-3.77 (m, 2 H), 3.90-3.98 (m, 2 H), 4.09-4.12 (m, 2 H), 4.17-4.23 (m, 2 H), 6.24-6.31 (m, 2 H), 10.76 (br s, 1 H).

6-(2-(dimethylamino)ethoxy)-4-fluoro-1-methyl-1'-(8-methyl-4-oxo-3,4,5,6,7,8-hexahydropyrido[2,3-d]pyrimidin-2-yl)spiro[indoline-3,4'-piperidin]-2-one (37d). To a solution of **34** (1 equiv, 35.0 mg, 0.1 mmol) in THF (1 mL) were added 2-(dimethylamino)ethanol (1.5 equiv, 15 µL, 0.15 mmol), ca. 2.2M diethyl azodicarboxylate in toluene (1.5 equiv, 68 µL, 0.15 mmol) and triphenylphosphine (1.5 equiv, 39.3 mg, 0.15 mmol) at ambient temperature. After stirring for 1 h, the mixture was diluted with water, extracted with ethyl acetate and washed with brine. The organic layer was dried over magnesium sulfate, filtered and evaporated under reduced pressure. The residue was column chromatographed on silica gel (methanol/ethyl acetate = 10:90) to give *tert*-butyl 6-(2-(dimethylamino)ethoxy)-4-fluoro-1-methyl-2-oxospiro[indoline-3,4'-piperidine]-1'-carboxylate (**35d**).

Compound **35d** was dissolved in chloroform (1 mL) and trifluoroacetic acid (130 equiv, 1 mL, 13 mmol) was added at ambient temperature. After stirring for 1 h, the

mixture was quenched with saturated sodium bicarbonate and extracted with chloroform. The organic layer was dried over magnesium sulfate, filtered and evaporated under reduced pressure. The residue was treated by general procedure A with **28** to give 11.6 mg (24%, 0.024 mmol) of **37d** as a white powder; LC-MS (ESI): m/z 485 ($M + H^+$). Retention time: 1.10 min. LC Purity: 99%. HRMS m/z ($M + H^+$) calculated for $C_{25}H_{33}FN_6O_3 + H^+$: 485.2676, found: 485.2675. ^{1}H NMR (400 MHz, $CDCl_3$) δ [ppm] 1.78-1.86 (m, 4H), 2.14-2.24 (m, 2H), 2.36 (s, 6H), 2.45 (t, J=6.3 Hz, 2H), 2.75 (t, J=5.6 Hz, 2H), 3.06 (s, 3H), 3.16 (s, 3H), 3.22-3.26 (m, 2H), 3.89-3.97 (m, 2H), 4.06 (t, J=5.6 Hz, 2H), 4.18-4.25 (m, 2H), 6.24-6.30 (m, 2H), 10.94 (br s, 1H).

4-fluoro-1-methyl-1'-(8-methyl-4-oxo-3,4,5,6,7,8-hexahydropyrido[2,3-d]pyrimidin-2-yl)-6-(2-(pyrrolidin-1-yl)ethoxy)spiro[indoline-3,4'-piperidin]-2-one (37e). The title compound was synthesized following the same procedure of **37d** as a white solid (21.6 mg, 42%); LC-MS (ESI): m/z 511 ($M + H^+$). Retention time: 1.12 min. LC Purity: >99%. HRMS m/z ($M + H^+$) calculated for $C_{27}H_{35}FN_6O_3 + H^+$: 511.2833, found: 511.2834. ^{1}H NMR (400 MHz, $CDCl_3$) δ [ppm] 1.79-1.88 (m, 8 H), 2.14-2.23 (m, 2H), 2.43-2.48 (m, 2H), 2.64-

2.74 (m, 4H), 2.92-2.98 (m, 2H), 3.07 (s, 3H), 3.16 (s, 3H), 3.22-3.27 (m, 2H), 3.88-3.97 (m, 2H), 4.10-4.22 (m, 4H), 6.25-6.30 (m, 2H), 10.55 (br s, 1H).

4-fluoro-1-methyl-1'-(8-methyl-4-oxo-3,4,5,6,7,8-hexahydropyrido[2,3-d]pyrimidin-2-yl)-6-(2-(piperidin-1-yl)ethoxy)spiro[indoline-3,4'-piperidin]-2-one (37f). The title compound was synthesized following the same procedure of **37d** as a white solid (19.0 mg, 36%); LC-MS (ESI): m/z 525 ($M + H^+$). Retention time: 1.14 min. LC Purity: 95%. HRMS m/z ($M + H^+$) calculated for $C_{28}H_{37}FN_6O_3 + H^+$: 525.2989, found: 525.2990. ^{1}H NMR (400 MHz, $CDCl_3$) δ [ppm] 1.43-1.50 (m, 2H), 1.60-1.67 (m, 4H), 1.79-1.88 (m, 4H), 2.14-2.23 (m, 2H), 2.44-2.59 (m, 6H), 2.77-2.83 (m, 2H), 3.07 (s, 3H), 3.16 (s, 3H), 3.23-3.28 (m, 2H), 3.88-3.97 (m, 2H), 4.08-4.18 (m, 4H), 6.24-6.29 (m, 2H).

4-fluoro-1-methyl-1'-(8-methyl-4-oxo-3,4,5,6,7,8-hexahydropyrido[2,3-d]pyrimidin-2-yl)-6-(2-morpholinoethoxy)spiro[indoline-3,4'-piperidin]-2-one (37g). The title compound was synthesized following the same procedure of **37d** as a white solid (11.0 mg, 21%); LC-MS (ESI): m/z 527 ($M + H^+$). Retention time: 1.10 min. LC Purity: >99%. HRMS m/z ($M + H^+$) calculated for $C_{27}H_{35}FN_6O_4 + H^+$: 527.2782, found: 527.2786. ^{1}H NMR (400 MHz, $CDCl_3$) δ [ppm] 1.79-1.88 (m, 4H), 2.15-2.23 (m, 2H), 2.44-2.49 (m, 2H), 2.56-2.60

(m, H), 2.78-2.83 (m, 2 H), 3.07 (s, H), 3.16 (s, 3H), 3.23-3.27 (m, 2H), 3.72-3.76 (m, 4H), 3.88-3.96 (m, 2H), 4.07-4.12 (m, 2H), 4.13-4.20 (m ,2H), 6.24-6.28 (m, 2H), 10.33 (br s, 1H).

4-fluoro-1-methyl-1'-(8-methyl-4-oxo-3,4,5,6,7,8-hexahydropyrido[2,3-d]pyrimidin-2-yl)-6-(2-(4-methylpiperazin-1-yl)ethoxy)spiro[indoline-3,4'-piperidin]-2-one (37h). The title compoundwas synthesized following the same procedure of **37d** as a white solid (6.0 mg, 11%); LC-MS (ESI): m/z 540 ($M + H^+$). Retention time: 1.25 min. LC Purity: 98%. HRMS m/z ($M + H^+$) calculated for $C_{28}H_{38}FN_7O_3 + H^+$: 540.3098, found: 540.3104. ^1H NMR (400 MHz, $CDCl_3$) δ [ppm] 1.78-1.87 (m, 4H), 2.14-2.23 (m, 2H), 2.31 (s, 3H), 2.42-2.69 (m, 10H), 2.80-2.84 (m, 2H), 3.07 (s, 3H), 3.16 (s, 3H), 3.23-3.27 (m, 2H), 3.88-3.96 (m, 2H), 4.06-4.11 (m, 2H), 4.13-4.20 (m ,2H), 6.23-6.28 (m, 2H), 10.32 (br s, 1H).

4-fluoro-1-methyl-1'-(8-methyl-4-oxo-3,4,5,6,7,8-hexahydropyrido[2,3-d]pyrimidin-2-yl)-6-((1-methylpiperidin-4-yl)oxy)spiro[indoline-3,4'-piperidin]-2-one (37i) . The title compound was synthesized following the same procedure of **37d** as a white solid (22.3 mg, 44%); LC-MS (ESI): m/z 511 ($M + H^+$). Retention time: 1.13 min. LC Purity: 98%.

HRMS m/z (M + H^+) calculated for $C_{27}H_{35}FN_6O_3$ + H^+: 511.2833, found: 511.2820. ^1H NMR (400 MHz, $CDCl_3$) δ [ppm] 1.79-1.90 (m, 6H), 1.98-2.06 (m, H), 2.14-2.23 (m, 2 H), 2.28-2.36 (m, 5H), 2.44-2.49 (m, 2H), 2.65-2.73 (m, 2H), 3.07 (s, 3H), 3.16 (s, 3H), 3.23-3.27 (m, 2H), 3.88-3.97 (m, 2H), 4.13-4.20 (m, 2H), 4.26-4.32 (m, 1H), 6.23-6.28 (m, 2H), 10.26 (br s, 1H).

2-((4-fluoro-1-methyl-1'-(8-methyl-4-oxo-3,4,5,6,7,8-hexahydropyrido[2,3-d]pyrimidin-2-yl)-2-oxospiro[indoline-3,4'-piperidin]-6-yl)oxy)acetic acid (37j). The title compound was synthesized following the same procedure of **37d** as a white powder (20.9 mg, 85%); LC-MS (ESI): m/z 472 (M + H^+). Retention time: 1.46 min. LC Purity: 97%. HRMS m/z (M + H^+) calculated for $C_{23}H_{26}FN_5O_5$ + H^+: 472.1996, found: 472.2003. ^1H NMR (400 MHz, DMSO-d_6) δ [ppm] 1.38-1.49 (m, 2 H), 1.72-1.81 (m, 2 H), 1.83-1.90 (m, 2 H), 2.49-2.54 (m, 2 H), 3.09 (s, 3 H), 3.14 (s, 3 H), 3.30-3.35 (m, 2 H), 3.77-3.94 (m, 4 H), 4.65 (s, 2 H), 6.22-6.28 (m, 2 H).

6-(Dimethylamino)-4-fluoro-1-methyl-1'-(8-methyl-4-oxo-3,4,5,6,7,8-hexahydropyrido[2,3-d]pyrimidin-2-yl)spiro[indoline-3,4'-piperidin]-2-one (41a).

41a. 1. To a solution of benzyl 6-bromo-4-fluoro-1-methyl-2-oxo-spiro[indoline-3,4'-piperidine]-1'-carboxylate (**42**, 1 equiv, 500 mg, 1.12 mmol) in toluene (8 mL) were added dimethylamine hydrochloride (2 equiv, 182 mg, 2.24 mmol), sodium *tert*-butoxide (3.5 equiv, 376 mg, 3.91 mmol), tris(dibenzylideneacetone) dipalladium(0) (0.1 equiv, 100 mg, 0.11 mmol) and BINAP (0.15 equiv, 111 mg, 0.168 mmol). After stirring under microwave condition (100 °C) for 1 h, the mixture was filtered and washed with ethyl acetate. The filtrate was evaporated under reduced pressure. The residue was column chromatographed on silica gel (ethyl acetate/n-hexane = 50:50) and fractions were evaporated to give 277 mg (0.67 mmol, 60%) of benzyl 6-(dimethylamino)-4-fluoro-1-methyl-2-oxospiro[indoline-3,4'-piperidine]-1'-carboxylate (Cbz-**40a**).

41a. 2. Compound Cbz-**40a** (1 equiv, 300 mg, 0.73 mmol) and palladium hydroxide on carbon (33% w/w, 100 mg) were suspended in ethanol (10 mL) and dichloromethane (10 mL). After stirring under a hydrogen atmosphere (~0.4 MPa), reaction mixture was filtered through a celite pad, and washed with ethanol-dichloromethane. The filtrate was evaporated under reduced pressure to give 239 mg (quant., 0.83 mmol) of 6-(dimethylamino)-4-fluoro-1-methylspiro[indoline-3,4'-piperidin]-2-one (**40a**).

41a. 3. Compound **40a** (1.0 equiv, 120 mg, 0.38 mmol), **28** (1.5 equiv, 115 mg, 0.58 mmol) and triethylamine (3.0 equiv, 0.15 ml, 1.15 mmol) were dispensed in a round vessel (10 mL) in ethanol (3 mL). The mixture was heated at 90 °C for 27 h. The reaction mixture was diluted with ethyl acetate and water. Aqueous layer was separated and extracted twice with ethyl acetate. Combined organic layer was washed with water and saturated sodium chloride solution, dried over sodium sulfate, filtered and evaporated under reduced pressure. The residue was purified by silica gel and then amino-silica gel column chromatography eluted with chloroform: methanol (v/v = 95: 5) to give 74 mg (44%, 0.17 mmol) of **41a** as a clear solid. LC-MS (ESI): m/z 441 ($M + H^+$). Retention Time: 1.34 min. Purity: 98%. HRMS m/z ($M + H^+$) calculated for $C_{23}H_{29}FN_6O_2 + H^+$: 441.2414, found: 441.2413. ^1H NMR (270 MHz, $CDCl_3$), δ: 1.73-1.85 (m, 8H), 2.24-2.62 (m, 6H), 2.88-3.05 (m, 2H), 3.33 (t, *J*= 5.4 Hz, 2H), 3.48 (s, 2H), 3.84 (t, *J*= 5.4 Hz, 2H), 6.31-6.41 (m, 2 H), 7.01-7.26 (m, 1H).

4-fluoro-1-methyl-1'-(8-methyl-4-oxo-3,4,5,6,7,8-hexahydropyrido[2,3-d]pyrimidin-2-yl)-6-(piperidin-1-yl)spiro[indoline-3,4'-piperidin]-2-one (41b). The title compound was synthesized following the same procedure of **41g** as a white solid (14.9 mg, 78%); LC-

MS (ESI): m/z 481 (M + H^+). Retention time: 1.25 min. LC Purity: 99%. HRMS m/z (M + H^+) calculated for $C_{26}H_{33}FN_6O_2$ + H^+: 481.2727, found: 481.2722. ^{1}H NMR (400 MHz, $CDCl_3$) δ [ppm] 1.57-1.64 (m, 2H), 1.66-1.73 (m, 4H), 1.78-1.87 (m, 4H), 2.10-2.20 (m, 2H), 2.42-2.47 (m, 2H), 3.06 (s, 3H), 3.15-3.27 (m, 9H), 3.91-3.99 (m, 2H), 4.14-4.22 (m, 2H), 6.18-6.24 (m, 2H), 10.88 (br s, 1H).

4-fluoro-1-methyl-1'-(8-methyl-4-oxo-3,4,5,6,7,8-hexahydropyrido[2,3-d]pyrimidin-2-yl)-6-(piperazin-1-yl)spiro[indoline-3,4'-piperidin]-2-one (41c).

41c. 1. To a solution of **34** (1 equiv, 175.2 mg, 0.5 mmol) in chloroform (2.5 mL) were added trifluoromethanesulfonic anhydride (1.5 equiv, 123 μL, 0.75 mmol) and triethylamine (3 equiv, 209 μL, 1.5 mmol) at 0 °C. After stirring at ambient temperature for 1 h, the mixture was quenched with saturated sodium bicarbonate and extracted with chloroform. The organic layer was dried over magnesium sulfate, filtered and evaporated under reduced pressure. The residue was column chromatographed on silica gel (ethyl acetate/n-hexane = 20:80) to give 159 mg (66%, 0.33 mmol) of *tert*-butyl 4-fluoro-1-methyl-2-oxo-6-(((trifluoromethyl)sulfonyl)oxy)spiro [indoline-3,4'-piperidine]-1'-carboxylate (**38**).

41c. 2. To a solution of **38** (48.2 mg, 0.1 mmol) in toluene (1.5 mL) were added benzyl piperazine-1-carboxylate (2 equiv, 44.1 mg, 0.2 mmol), cesium carbonate (1.5 equiv, 48.9 mg, 0.15 mmol), palladium(II) acetate (0.3 equiv, 6.7 mg, 0.03 mmol) and BINAP (0.3 equiv, 18.7 mg, 0.03 mmol). After stirring at reflux for 22 h, the mixture was quenched with water and filtered through a celite pad. The filtrate was extracted with ethyl acetate and washed with brine. The organic layer was dried over magnesium sulfate, filtered and evaporated under reduced pressure. The residue was column chromatographed on silica gel (ethyl acetate/n-hexane = 50:50) to give 51.8 mg (94%, 0.094 mmol) of *tert*-butyl 6-(4-(benzyloxycarbonyl)piperazin-1-yl)-4-fluoro-1-methyl-2-oxospiro[indoline-3,4'-piperidine]-1'-carboxylate (**39c**).

41c. 3. Compound **39c** (1 equiv, 51.8 mg, 0.094 mmol) was dissolved in chloroform (1 mL) and trifluoroacetic acid (138 equiv, 1 mL, 13 mmol) was added at ambient temperature. After stirring for 1 h, the mixture was quenched with saturated sodium bicarbonate and extracted with chloroform. The organic layer was dried over magnesium sulfate, filtered and evaporated under reduced pressure.

41c. 4. The residue was treated by general procedure A with **28** to give 24.4 mg (42%, 0.040 mmol) of benzyl 4-(4-fluoro-1-methyl-1'-(8-methyl-4-oxo-3,4,5,6,7,8-hexahydropyrido[2,3-*d*]pyrimidin-2-yl)-2-oxospiro[indoline-3,4'-piperidin]-6-yl)piperazine-1-carboxylate (Cbz-**41c**). **41c. 5.** Cbz-**41c** was treated by general procedure B to give 13.5 mg (84%, 0.028 mmol) of **41c** as an off-white solid; LC-MS (ESI): m/z 417 ($M + H^+$). Retention time: 1.10 min. LC Purity: 99%. HRMS m/z ($M + H^+$) calculated for $C_{25}H_{32}FN_7O_2 + H^+$: 482.2680, found: 482.2671. ^{1}H-NMR (400 MHz, $CDCl_3$) δ: 1.82-2.02 (m, 4H), 2.08-2.23 (m, 2H), 2.51-2.62 (m, 2), 3.18-3.26 (m, 6H), 3.33-3.41 (m, 2H), 3.47-3.58 (m, 6H), 3.96-4.08 (m, 4H), 4.11-4.24 (m, 2H), 6.40-6.61 (m, 2H).

4-fluoro-1-methyl-1'-(8-methyl-4-oxo-3,4,5,6,7,8-hexahydropyrido[2,3-d]pyrimidin-2-yl)-6-(4-methylpiperazin-1-yl)spiro[indoline-3,4'-piperidin]-2-one (41d). The title compound was synthesized following the same procedure of **41g** as a white solid (31.5 mg, 64%); LC-MS (ESI): m/z 496 ($M + H^+$). Retention time: 1.08 min. LC Purity: 98%. HRMS m/z ($M + H^+$) calculated for $C_{26}H_{34}FN_7O_2 + H^+$: 496.2836, found: 496.2833. ^{1}H NMR (400 MHz, $CDCl_3$) δ [ppm] 1.80-1.87 (m, 4 H), 2.11-2.20 (m, 2H), 2.36 (s, 3H), 2.44-2.49 (m,

2H), 2.55-2.60 (m, 4H), 3.07 (s, 3H), 3.17 (s, 3H), 3.21-3.27 (m, 6H), 3.89-3.98 (m, 2H), 4.10-4.17 (m, 2H), 6.19-6.25 (m, 2H), 10.32 (br s, 1H).

6-(cis-3,5-dimethylpiperazin-1-yl)-4-fluoro-1-methyl-1'-(8-methyl-4-oxo-3,4,5,6,7,8-hexahydropyrido[2,3-d]pyrimidin-2-yl)spiro[indoline-3,4'-piperidin]-2-one (41e). The title compound was synthesized following the same procedure of **41c** as a white solid (27.8 mg, 73%); LC-MS (ESI): m/z 510 ($M + H^+$). Retention time: 1.12 min. LC Purity: 98%. HRMS m/z ($M + H^+$) calculated for $C_{27}H_{36}FN_7O_2 + H^+$: 510.2993, found: 510.2996. ^1H NMR (400 MHz, $CDCl_3$) δ [ppm] 1.17 (d, J=6.0 Hz, 6H), 1.80-1.90 (m, 4H), 2.10-2.20 (m, 2H), 2.30-2.50 (m, 4H), 2.95-3.05 (m, 2H), 3.07 (s, 3H), 3.19 (s, 3H), 3.20-3.30 (m, 2H), 3.45-3.55 (m, 2H), 3.90-4.00 (m, 2H), 4.10-4.20 (m, 2H), 6.15-6.25 (m, 2H).

4-fluoro-1-methyl-1'-(8-methyl-4-oxo-3,4,5,6,7,8-hexahydropyrido[2,3-d]pyrimidin-2-yl)-6-morpholinospiro[indoline-3,4'-piperidin]-2-one (41f). The title compound was synthesized following the same procedure of **41g** as a white solid (30.1 mg, 62%); LC-MS (ESI): m/z 483 ($M + H^+$). Retention time: 1.32 min. LC Purity: >99%. HRMS m/z ($M + H^+$) calculated for $C_{25}H_{31}FN_6O_3 + H^+$: 483.2520, found: 483.2518. ^1H NMR (400 MHz, $CDCl_3$): 1.79-1.88 (m, 4H), 2.12-2.21 (m, 2H), 2.44-2.49 (m, 2H), 3.07 (s, 3H), 3.15-3.21

(m, 7H), 3.22-3.27 (m, 2H), 3.83-3.88 (m, 4H), 3.90-3.98 (m, 2H), 4.12-4.20 (m, 2H), 6.17-6.24 (m, 2H), 10.44 (br s, 1H).

6-(cis-2,6-dimethylmorpholino)-4-fluoro-1-methyl-1'-(8-methyl-4-oxo-3,4,5,6,7,8-hexahydropyrido[2,3-d]pyrimidin-2-yl)spiro[indoline-3,4'-piperidin]-2-one (41g).

41g.1. To a solution of **38** (1 equiv, 48.2 mg, 0.1 mmol) in toluene (1 mL) were added cis-2,6-dimethylmorpholine (1.2 equiv, 15 μL, 0.12 mmol), cesium carbonate (1.5 equiv, 48.9 mg, 0.15 mmol), palladium(II) acetate (0.1 equiv, 2.2 mg, 0.01 mmol) and BINAP (0.1 equiv, 6.2 mg, 0.01 mmol). After stirring at reflux for 14 h, the mixture was quenched with water and filtered through a celite pad. The filtrate was extracted with ethyl acetate and washed with brine. The organic layer was dried over magnesium sulfate, filtered and evaporated under reduced pressure. The residue was column chromatographed on silica gel (ethyl acetate/n-hexane = 50:50) to give 18.2 mg (41%, 0.041 mmol) of *tert*-butyl 6-(cis-2,6-dimethylmorpholino)-4-fluoro-1-methyl-2-oxospiro[indoline-3,4'-piperidine]-1'-carboxylate (**39g**). ^{1}H-NMR (400 MHz, $CHCl_3$) δ: 1.27 (d, *J*=6.2 Hz, 6H), 1.49 (s, 9H), 1.70-1.77 (m, 2H), 2.01-2.11 (m, 2H), 2.41-2.49 (m, 2H), 3.17 (s, 3H), 3.40-3.45 (m, 2H), 3.68-3.94 (m, 6H), 6.15-6.23 (m, 2H).

41g. 2. Compound **39g** (1 equiv, 29.9 mg, 0.067 mmol) was dissolved in chloroform (1 mL) and trifluoroacetic acid (200 equiv, 1 mL, 13 mmol) was added at ambient temperature. After stirring for 1 h, the mixture was quenched with saturated sodium bicarbonate and extracted with chloroform. The organic layer was dried over magnesium sulfate, filtered and evaporated under reduced pressure.

41g. 3. The residue was treated by general procedure A with **28** to give 22.6 mg (66%, 0.044 mmol) of **41g** as a white powder. LC-MS (ESI): m/z 511 ($M + H^+$). LC Purity: 99%. HRMS m/z ($M + H^+$) calculated for $C_{27}H_{35}FN_6O_3 + H^+$: 511.2833, found: 511.2825. ^1H NMR (400 MHz, $CDCl_3$), δ: 1.27 (d, J=6.2 Hz, 6H), 1.79-1.87 (m, 4H), 2.11-2.20 (m, 2H), 2.42-2.49 (m, 4H), 3.07 (s, 3H), 3.19 (s, 3H), 3.23-3.27 (m, 2H), 3.40-3.45 (m, 2H), 3.73-3.82 (m, 2H), 3.89-3.97 (m, 2H), 4.07-4.15 (m, 2H), 6.16-6.23 (m, 2H).

Physicochemical and biochemical properties evaluation. Aqueous solubility, PAMPA, protein binding assay, liver microsomal stability assay, and P-glycoprotein efflux assay were performed according to the protocol described in the previous report.[21]

Pharmacokinetic Analysis. The pharmacokinetic (PK) analyses of mouse intraperitoneal (ip, 20 mg/kg), rat per oral (po, 3 mg/kg) and intravenous (iv, 3 mg/kg)

administrations were performed in Meiji Seika pharmaceutical and Nemoto Science Co. Ltd. according to the standard protocols described in the previous report[21] under previous approval from the Animal Care and Ethic Committee of these companies.

Biological Evaluation. Preparation of tankyrase and PARP family proteins. FLAG-tagged tankyrase-1 (TNKS) and -2 (TNKS2) proteins were prepared by the method described in the previous report.[20] Human PARP1 and PARP2 were purchased from Trevigen, Gaithersburg, MD 20877 and Bioscience, San Diego, CA 92121 USA, respectively. The catalytic domain of human PARP10 (residues 818–1025) were prepared by the method described in the previous report.[21]

ELISA for tankyrases, PARP1, PARP2, and PARP10. To measure poly (ADP-ribosyl)ation activity of tankyrases, the auto-poly (ADP-ribosyl)ation reaction of tankyrase-1 (TNKS) and -2 (TNKS2) proteins was conducted using an ELISA. FLAG-tagged tankyrase-1 [~2 μg in phosphate-buffered saline (PBS)] or tankyrase-2 (~0.5 μg in PBS) was bound to Nunc-Immuno MaxiSorp 96-well plates (ThermoFisher Scientific, Waltham, MA, USA) overnight at 4°C. After washing the plates four times with 200 μL of washing buffer (PBS containing 0.1% Triton X-100), 200 μL of Blocking One (Nacalai

Tesque, Kyoto, Japan) was added. After 1 h at room temperature, the plates were washed four times with 200 μL of washing buffer. Then, a test compound in PARP buffer [50 mM Tris-HCl (pH 8.0), 4 mM $MgCl_2$, 0.2 mM dithiothreitol] was added to each well and incubated for 10 min at room temperature. The auto-PARylation reaction was initiated by adding 25 μM NAD^+ containing 10% biotinylated-NAD^+ (Trevigen, Gaithersburg, MD, USA) in the 50 μL reaction mixture for 45 min at 30°C. After washing the plates four times with 200 μL of washing buffer, 50 μL of Strep-HRP (Trevigen) (1:5000, diluted with PBS) was added and the plates were incubated for 20 min at room temperature. Subsequently, the plates were washed four times with the washing buffer and 50 μL of ELISA POD substrate TMB solution (Nacalai Tesque) was added. After 30-min incubation at room temperature, the absorbance (630 nm) was measured with a SpectraMax 340PC microplate reader (Molecular Devices, San Jose, CA, USA). A blank value (in the absence of enzymes) was subtracted before calculating percent inhibition. To measure poly- or mono(ADP-ribosyl)ation activity of PARP1, PARP2, or PARP10, an ELISA was performed as described in the previous report.[21]

Cell culture. A human colorectal cancer cell line COLO-320DM was maintained in RPMI1640 medium (Nacalai Tesque or Wako) with 10% heat-inactivated fetal bovine serum (FBS) as described previously.[20] Human colorectal cancer cell lines RKO and DLD-1 and human embryonic kidney cell line HEK293 were maintained in DMEM medium (Nacalai Tesque or Wako) with 10% FBS as described previously.[17] All human colorectal cancer cell lines were obtained from the American Type Culture Collection (Manassas, VA, USA). The cell lines COLO-320DM and RKO were authenticated by short tandem repeat profiling analysis (BEX, Tokyo, Japan) in 2016.

TCF reporter assay. TCF reporter assay was carried out using DLD-1 and HEK293 cells transfected with the β-catenin-responsive reporter vector pTcf7wt-luc provided by Dr. Kunitada Shimotohno (National Center for Global Health and Medicine, via RIKEN BioResource Center, Ibaraki, Japan) as described previously.[21]

COLO-320DM cell growth inhibition CellTiter-Glo assay. To evaluate cell viability, CellTiter-Glo® reagent was used after treatment of cells with compounds at a final DMSO concentration of 1% (v/v) for 4 days. Cell viability was determined by

measurement of luminescence monochromator, Synergy H4 Hybrid Reader (BioTek, Japan) as described previously.[21]

MTT cell proliferation assay. To evaluate cell viability, the cells treated with compounds for 5 days were incubated with thiazol blue tetrazolium bromide (MTT) at a final concentration of 1 mg/mL at 37°C for 4 h. Then the medium containing MTT was removed and dimethyl sulfoxide was added to the cells. Following that optical density at 570 nm and 630 nm for reference was measured using an xMark microplate spectrophotometer (Bio-RAD, Hercules, CA, USA) as described previously.[20]

In vivo xenograft experiments. Animal experiments were performed as described previously.[20] COLO-320DM cells were suspended in Matrigel (Corning, Corning, NY, USA) and Hanks' balanced salt solution in a 1:1 ratio (5.2×10^6 cells/100 μL/mouse) and were implanted subcutaneously in the rear right flank of 6-week-old female NOD.CB17-*Prkdc*^{scid}/J mice (Charles River Laboratories Japan, Inc., Kanagawa, Japan). The length (L) and width (W) of the tumor mass were measured, and the tumor volume (TV) was calculated using the equation: $TV = (L \times W^2)/2$. When tumor volumes reached approximately 100 mm^3 (86–118 mm^3 and 78–113 mm^3 for intraperitoneal and

oral administration, respectively), mice were separated into groups of 10 animals for intraperitoneal and oral administration, respectively, with similarly sized tumors, and treatment was initiated the day after grouping. For intraperitoneal administration, dosing solution contained 15% dimethyl sulfoxide, 17.5% Cremophor, 8.75% ethanol, 8.75% PEG-40 hydrogenated castor oil and 50% phosphate buffered saline. For oral administration, **41g** was milled and suspended in sterilized 0.5% (w/v) methyl cellulose in water. Tumor growth inhibition coefficient (% TGI) was calculated according to the following equation: % TGI = $[(V_{vehicle}-V_{experiment})/V_{vehicle}] \times 100$, where V is relative tumor volume at the final day.

Western blot analysis. Cells were harvested and the cell lysates were prepared with a lysis buffer (50 mM Tris-HCl, pH 8.0, 150 mM NaCl, 1% Nonidet P-40) containing 0.125 mM dithiothreitol, 2% (v/v) of a protease inhibitor cocktail (Nacalai Tesque) and 1% (v/v) of a phosphatase inhibitor cocktail (Nacalai Tesque). Western blot analysis was performed as previously described.[20] The primary antibodies used were anti-tankyrase-1/2 (H350; Santa Cruz Biotechnology, 0.4 μg/mL), anti-active β-catenin (8E7; Millipore, Darmstadt, Germany, 2 μg/mL), anti-β-catenin (6B3; Cell Signaling Technology,

Danvers, MA, USA, 1:500), anti-Axin1 (C76H11; Cell Signaling Technology, 1:500), anti-Axin2 (76G6; Cell Signaling Technology, 1:500) and anti-glyceraldehyde 3-phosphate dehydrogenase (GAPDH) (6C5; Fitzgerald, Acton, MA, USA, 0.66 μg/mL).

Tumor protein isolation. From each group four tumors which have nearly average volumes of the group were subjected to western blot analysis. Cytosolic and nuclear proteins were extracted from minced frozen tumor tissues by using a CelLytic NuCLEAR Extraction Kit (Sigma) according to the manufacturer's instructions.

Crystal structure determination. The PARP catalytic domain of human TNKS2 (residues 946–1162) was prepared as described previously.[21] Crystals of human TNKS2 were obtained by the sitting drop method at 277 K, where the protein solution was mixed with the reservoir solution containing 100 mM Tris-HCl buffer (pH 8.5) and 1.60–1.65 M diammonium hydrogen phosphate. Crystals were soaked into the reservoir solution containing 1 mM inhibitor for seven days, before flash-cooled in liquid nitrogen using 20% glycerol as the cryoprotectant. Diffraction data were collected at the BL26B2 beamline of SPring-8 (Harima, Japan), and were processed with XDS[40] and the CCP4 suite[41]. The initial phases were calculated by rigid-body refinement with PHENIX[42] using

the structurally conserved portion of a previously determined structure (PDB ID: 5ZQP).[21] The topology and parameter file for the inhibitor was generated with eLBOW[43] from SMILES strings. Further structure refinement was performed using PHENIX with manual model building using COOT[44]. Crystallographic statistics are summarized in Supporting Information Table S7. The coordinates and structure factors have been deposited at the Protein Data Bank with the accession code 6KRO.

■ ASSOCIATED CONTENT

Supporting Information is available free of charge on the ACS Publications website at http://pubs.acs.org. Additional figures illustrating data of western blot analysis, mouse and rat pharmacokinetics, biological assays and superimposed complex structure of **41g** and Olaparib, experimental procedures and analytical data for final compounds, and *in vitro* biological assay data with SD were listed. (pdf)

Molecular formula strings and some data (csv)

Accession Codes Coordinates and structure factors have been deposited at the Protein Data Bank with the code 6KRO. Authors will release the atomic coordinates upon article publication.

■ AUTHOR INFORMATION

Corresponding Author

*F.Shirai: phone, +81484678792; e-mail, fumiyuki.shirai@riken.jp.

*H.Koyama: phone, +81484679253; e-mail, hiroo.koyama@riken.jp.

■ ACKNOWLEDGEMENTS

We thank Fumiko Kyotani, Satsuki Irie, and Dr. Takayoshi Nakaoka for helping evaluate the aqueous solubilities of compounds, PAMPA, and microsomal stability experiments. We recognize Dr. Takemichi Nakamura for his assistance in high-resolution mass spectrometry. We also acknowledge Dr. Hiroaki Ohtake and Shinya Kohno for their technical support. This research was supported by RIKEN Program for Drug Discovery and Medical Technology Platforms and Japan Agency for Medical Research and Development (AMED) under Grant Numbers 15cm0106004 (to M.Y.), JP15cm0106030 (to H.S. and Y.Y.) and JP16cm0106102, JP17cm0106102, JP18cm0106102 (to H.S. and Y.Y.).

■ DEDICATION

This article is dedicated to the memory of Dr. Kenji Mori (1935-2019), an adviser of Drug Discovery Chemistry Platform Unit (2013-2019), professor emeritus of the University of Tokyo, and a member of the Japan Academy (2015-2019).

■ ABBREVIATIONS USED

ADME, absorption, distribution, metabolism and excretion ; APC, adenomatous polyposis coli; AXIN, axis inhibition protein; AUC, area under the curve; bid, twice daily; CRC, colorectal cancer; C_{max}, maximum concentration; CYP, cytochrome P450 ; ELISA, enzyme-linked immunosorbent assay; ER, efflux ratio; GI_{50}, half maximal growth inhibition; IC_{50}, half maximal inhibitory concentration; IP, intraperitoneal; MDCK II, Madin-Darby canine kidney cell II; MDR1, multiple drug resistance 1; MTPP, 8-methyl-5,6,7,8-tetrahydropyrido[2,3-*d*]pyrimidin-4(7*H*)-one; NER, net efflux ratio; NOD-SCID, non-obese diabetic mice with severe combined immunodeficiency disease; PAMPA, parallel artificial membrane permeability assay; PBS, phosphate buffered salts; PARP, poly(ADP-ribose) polymerase; PARsylation, poly-ADP-ribosylation; P-gp, P-glycoprotein; TCF, T-cell factor ; PO, per oral; TGI, tumor growth inhibition; TNKS,

telomere-associated poly(ADP-ribose) polymerase tankyrase; WNT, wingless and its vertebrate ortholog.

REFERENCES

1. American Institute for Cancer Research Home Page. (accessed Jun 10, 2020) https://www.wcrf.org/dietandcancer/cancer-trends/colorectal-cancer-statistics
2. Cancer Genome Atlas Network. Comprehensive molecular characterization of human colon and rectal cancer. *Nature* **2012**, *487*, 330-337.
3. Yaeger, R.; Chatila, W. K.; Lipsyc, M. D.; Hechtman, J. F.; Cercek, A.; Sanchez-Vega, F.; Jayakumaran, G.; Middha, S.; Zehir, A.; Donoghue, M. T. A.; You, D.; Viale, A.; Kemeny, N.; Segal, N. H.; Stadler, Z. K.; Varghese, A. M.; Kundra, R.; Gao, J.; Syed, A.; Hyman, D. M.; Vakiani, E.; Rosen, N.; Taylor, B. S.; Ladanyi, M.; Berger, M. F.; Solit, D. B.; Shia, J.; Saltz, L.; Schultz, N. Clinical sequencing defines the genomic landscape of metastatic colorectal cancer. *Cancer Cell* **2018**, *33*, 125-136.
4. Chiang, Y. J.; Hsiao, S. J.; Yver, D.; Cushman, S. W.; Tessarollo, L.; Smith, S.; Hodes, R. J. Tankyrase 1 and tankyrase 2 are essential but redundant for mouse embryonic development. *PLoS One.* **2008**, *3*, e2639.

5. Huang, S. M.; Mishina, Y. M.; Liu, S.; Cheung, A.; Stegmeier, F.; Michaud, G. A.; Charlat, O.; Wiellette, E.; Zhang, Y.; Wiessner, S.; Hild, M.; Shi, X.; Wilson, C. J.; Mickanin, C.; Myer, V.; Fazal, A.; Tomlinson, R.; Serluca, F.; Shao, W.; Cheng, H.; Shultz, M.; Rau, C.; Schirle, M.; Schlegl, J.; Ghidelli, S.; Fawell, S.; Lu, C.; Curtis, D.; Kirschner, M. W.; Lengauer, C.; Finan, P. M.; Tallarico, J. A.; Bouwmeester, T.; Porter, J. A.; Bauer, A.; Cong, F. Tankyrase inhibition stabilizes axin and antagonizes Wnt signalling. *Nature* **2009,** *461*, 614-620.

6. Schatoff, E. M.; Goswami, S.; Zafra, M. P.; Foronda, M.; Shusterman, M.; Leach, B. I.; Katti, A.; Diaz, B. J.; Dow, L. E. Distinct CRC-associated APC mutations dictate response to tankyrase inhibition. *Cancer Discov.* **2019,** pii: CD-19-0289. doi: 10.1158/2159-8290.

7. Tanaka, N.; Mashima, T.; Mizutani, A.; Sato, A.; Aoyama, A.; Gong, B.; Yoshida, H.; Muramatsu, Y.; Nakata, K.; Matsuura, M.; Katayama, R.; Nagayama, S.; Fujita, N.; Sugimoto, Y.; Seimiya, H. APC mutations as a potential biomarker for sensitivity to tankyrase inhibitors in colorectal cancer. *Mol Cancer Ther.* **2017,** *16*, 752-762.

8. Smith, S.; de Lange, T. Tankyrase promotes telomere elongation in human cells. *Curr. Biol.* **2000,** *10*, 1299-1302.

9. Wang, W.; Li, N.; Li, X.; Tran, M. K.; Han, X.; Chen, J. Tankyrase inhibitors target YAP by stabilizing angiomotin family proteins. *Cell Rep.* **2015,** *13*, 524-532.

10. Smith, S.; de Lange, T. Cell cycle dependent localization of the telomeric PARP, tankyrase, to nuclear pore complexes and centrosomes. *J. Cell Sci.* **1999,** *112*, 3649-3656.

11. Chi, N. W.; Lodish, H. F. Tankyrase is a golgi-associated mitogen-activated protein kinase substrate that interacts with IRAP in GLUT4 vesicles. *J. Biol. Chem.* **2000,** *275*, 38437-38444.

12. Thorvaldsen, T. E. Targeting tankyrase to fight WNT-dependent tumors. *Basic Clin. Pharmacol. Toxicol.* **2017,** *121*, 81-88.

13. Mariotti, L.; Pollock, K.; Guettler, S. Regulation of Wnt/β-catenin signalling by tankyrase-dependent poly(ADP-ribosyl)ation and scaffolding. *Br. J. Pharmacol.* **2017,** *174*, 4611-4636.

14. Ferri, M.; Liscio, P.; Carotti, A.; Asciutti, S.; Sardella, R.; Macchiarulo, A.; Camaioni, E. Targeting Wnt-driven cancers: Discovery of novel tankyrase inhibitors. *Eur. J. Med. Chem.* **2017,** *142*, 506-522.

15. Narwal, M.; Venkannagari, H.; Lehtiö, L. Structural basis of selective inhibition of human tankyrases. *J. Med.Chem.* **2012**, *55*, 1360-1367.

16. Gunaydin, H.; Gu, Y.; Huang, X. Novel binding mode of a potent and selective tankyrase inhibitor. *Plos One* **2012**, *7*, e33740-e33740.

17. Voronkov, A.; Holsworth, D. D.; Waaler, J.; Wilson, S. R.; Ekblad, B.; Perdreau-Dahl, H.; Dinh, H.; Drewes, G.; Hopf, C.; Morth, J. P.; Krauss, S. Structural basis and SAR for G007-LK, a lead stage 1,2,4-triazole based specific tankyrase 1/2 inhibitor. *J. Med. Chem.* **2013,** *56*, 3012-3023.

18. Karlberg, T.; Markova, N.; Johansson, I.; Hammarström, M.; Schütz, P.; Weigelt, J.; Schüler, H. Structural basis for the interaction between tankyrase-2 and a potent Wnt-signaling inhibitor. *J. Med. Chem.* **2010,** *53*, 5352-5355.

19. Kirby, C.A.; Cheung, A.; Fazal, A.; Shultz, M.D.; Stams, T. Structure of human tankyrase 1 in complex with small-molecule inhibitors PJ34 and XAV939. *Acta Cryst., Sect. F.* **2012,** *68*, 115-118

20. Mizutani, A.; Yashiroda, Y.; Muramatsu, Y.; Yoshida, H.; Chikada, T.; Tsumura, T.; Okue, M.; Shirai, F.; Fukami, T.; Yoshida, M.; Seimiya, H. RK-287107, a potent and specific tankyrase inhibitor, blocks colorectal cancer cell growth in a preclinical model. *Cancer Sci.* **2018**, *109*, 4003-4014.

21. Shirai, F.; Tsumura, T.; Yashiroda, Y.; Yuki, H.; Niwa, H.; Sato, S.; Chikada, T.; Koda, Y.; Washizuka, K.; Yoshimoto, N.; Abe, M.; Onuki, T.; Mazaki, Y.; Hirama, C.; Fukami, T.; Watanabe, H.; Honma, T.; Umehara, T.; Shirouzu, M.; Okue, M.; Kano, Y.; Watanabe, T.; Kitamura, K.; Shitara, E.; Muramatsu, Y.; Yoshida, H.; Mizutani, A.; Seimiya, H.; Yoshida, M.; Koyama, H. Discovery of novel spiroindoline derivatives as selective tankyrase inhibitors. *J. Med. Chem.* **2019,** *62*, 3407-3427.

22. Shultz, M. D.; Cheung, A. K.; Kirby, C. A.; Firestone, B.; Fan, J.; Chen, C. H.; Chen, Z.; Chin, D. N.; Dipietro, L.; Fazal, A.; Feng, Y.; Fortin, P. D.; Gould, T.; Lagu, B.; Lei, H.; Lenoir, F.; Majumdar, D.; Ochala, E.; Palermo, M. G.; Pham, L.; Pu, M.;

Smith, T.; Stams, T.; Tomlinson, R. C.; Touré, B. B.; Visser, M.; Wang, R. M.; Waters, N. J.; Shao, W. Identification of NVP-TNKS656: The use of structure-efficiency relationships to generate a highly potent, selective, and orally active tankyrase inhibitor. *J. Med. Chem.* **2013,** *56*, 6495-6511.

23. Lau, T.; Chan, E.; Callow, M.; Waaler, J.; Boggs, J.; Blake, R. A.; Magnuson, S.; Sambrone, A.; Schutten, M.; Firestein, R.; Machon, O.; Korinek, V.; Choo, E.; Diaz, D.; Merchant, M.; Polakis, P.; Holsworth, D. D.; Krauss, S.; Costa, M. A novel tankyrase small-molecule inhibitor suppresses APC mutation-driven colorectal tumor growth. *Cancer Res.* **2013,** *73*, 3132-3144.

24. Zhong, Y.; Katavolos, P.; Nguyen, T.; Lau, T.; Boggs, J.; Sambrone, A.; Kan, D.; Merchant, M.; Harstad, E.; Diaz, D.; Costa, M.; Schutten, M. Tankyrase inhibition causes reversible intestinal toxicity in mice with a therapeutic index < 1. *Toxicol. Pathol.* **2016,** *44*, 267-278.

25. Jones, M. L.; Lilly, J. C.; Ankala, S. V.; Singleton, S. F. Heterocyclic compounds as antibiotic potentiators. PCT Int. Appl., 2016094730, Jun 16 2016.

26. Van Horn, K. S.; Burda, W. N.; Fleeman, R.; Shaw, L. N.; Manetsch, R. Antibacterial activity of a series of N2,N4-disubstituted quinazoline-2,4-diamines. *J. Med. Chem.* **2014**, *57*, 3075– 3093.

27. Xie, H.; Zeng, L.; Zeng, S.; Lu, X.; Zhang, G.; Zhao, X.; Cheng, N.; Tu, Z.; Zhiyuan Li, Z.; Xu, H.; Yang, L.; Zhang, X.; Huang, M.; Zhao, J.; Hu, W. Novel pyrrolopyrimidine analogues as potent dipeptidyl peptidase IV inhibitors based on pharmacokinetic property-driven optimization. *Eur. J. Med. Chem.* **2012**, *52*, 205-212.

28. Mistry, P.; Stewart, A. J.; Dangerfield, W.; Okiji, S.; Liddle, C.; Bootle, D.; Plumb, J. A.; Templeton, D.; Charlton, P. In vitro and in vivo reversal of P-glycoprotein-mediated multidrug resistance by a novel potent modulator, XR9576. *Cancer Res.* **2001,** *61*, 749-758.

29. Phoenix WinNonlin ver. 8.1.0, 2018; Certara, L.P.; 210 North Tucker Boulevard Suite 350, St. Louis, MO 63101 USA.

30. Alam, A.; Kowal, J.; Broude, E.; Roninson, I.; Locher, K. P. Structural insight into substrate and snhibitor discrimination by human P-glycoprotein. *Science* **2019**, *363*, 753–756.

31. Gu, C.; Lamb, M. L.; Johannes, J. W.; Sylvester, M. A.; Eisman, M. S.; Harrison, R. A.; Hu, H.; Kazmirski, S.; Mikule, K.; Peng, B. Modulating the strength of hydrogen bond acceptors to achieve low Caco2 efflux for oral bioavailability of PARP Inhibitors blocking centrosome clustering. *Bioorg. Med. Chem. Lett.* **2016,** *26*, 4775–4780.

32. Frézard, F.; Pereira-Maia, E.; Quidu, P.; Priebe, W.; Garnier-Suillerot, A. P-glycoprotein preferentially effluxes anthracyclines containing free basic versus charged amine. *Eur. J. Biochem.* **2001**, *268*, 1561–1567.

33. Kunikawa, S.; Tanaka, A.; Mukoyoshi, K.; Nagashima, S.; Tominaga, H.; Chida, N.; Tasaki, M.; Shirai, F. Optimization of 2,4-diamino-5-fluoropyrimidine derivatives as protein kinase C theta inhibitors with mitigated time-dependent drug–drug interactions and P-gp liability. *Bioorg. Med. Chem.* **2015,** *23*, 3269–3277.

34. Mashima, T.; Taneda, Y.; Jang, M.K.; Mizutani, A.; Muramatsu, Y.; Yoshida, H.; Sato, A.; Tanaka, N.; Sugimoto, Y.; Seimiya, H. mTOR signaling mediates resistance to tankyrase inhibitors in Wnt-driven colorectal cancer. *Oncotarget*, **2017,** *8*, 47902-47915.

35. Quackenbush, K. S.; Bagby, S.; Tai, W. M.; Messersmith, W. A.; Schreiber, A.; Greene, J.; Kim, J.; Wang, G.; Purkey, A.; Pitts, T. M.; Nguyen, A.; Gao, D.; Blatchford, P.; Capasso, A.; Schuller, A. G.; Eckhardt, S. G.; Arcaroli, J. J. The novel tankyrase inhibitor (AZ1366) enhances irinotecan activity in tumors that exhibit elevated tankyrase and irinotecan resistance. *Oncotarget* **2016,** *7*, 28273-28785.

36. Scarborough, H. A.; Helfrich, B. A.; Casás-Selves, M.; Schuller, A. G.; Grosskurth, S. E.; Kim, J.; Tan, A. C.; Chan, D. C.; Zhang, Z.; Zaberezhnyy, V.; Bunn, P. A.; DeGregori, J. AZ1366: An inhibitor of tankyrase and the canonical Wnt pathway that limits the persistence of non-small cell lung cancer cells following EGFR inhibition. *Clin. Cancer Res.* **2017,** *23*, 1531-1541.

37. Arqués, O.; Chicote, I.; Puig, I.; Tenbaum, S. P.; Argilés, G.; Dienstmann, R.; Fernández, N.; Caratù, G.; Matito, J.; Silberschmidt, D.; Rodon, J.; Landolfi, S.; Prat, A.; Espín, E.; Charco, R.; Nuciforo, P.; Vivancos, A.; Shao, W.; Tabernero, J.; Palmer, H. G. Tankyrase inhibition blocks Wnt/β-catenin pathway and reverts resistance to PI3K and AKT inhibitors in the treatment of colorectal cancer. *Clin. Cancer Res.* **2016,** *22*, 644-656.

38. Ha, G. H.; Kim, D. Y.; Breuer, E.K.; Kim, C. K. Combination treatment of polo-like linase 1 and tankyrase-1 inhibitors enhances anticancer effect in triple-negative breast cancer cells. *Anticancer Res.* **2018,** *38*, 1303-1310.

39. Menon, M.; Elliott, R.; Bowers. L.; Balan, N.; Rafiq, R.; Costa-Cabral, S.; Munkonge, F.; Trinidade, I.; Porter, R.; Campbell, A. D.; Johnson, E. R.; Esdar, C.; Buchstaller, H.-P.; Leuthner, B.; Rohdich, F.; Schneider, R.; Sansom, O.; Wienke, D.; Ashworth, A.; Lord, C. J. A novel tankyrase inhibitor, MSC2504877, enhances the effects of clinical CDK4/6 inhibitors. *Sci Rep.* **2019,** *9*, 201.

40. Kabsch, W. XDS. *Acta Cryst.* **2010,** *D66*, 125-132.

41. Winn, M. D.; Ballard, C. C.; Cowtan, K. D.; Dodson, E. J.; Emsley, P.; Evans, P. R.; Keegan, R. M.; Krissinel, E. B.; Leslie, A. G.; McCoy, A.; McNicholas, S. J.; Murshudov, G. N.; Pannu, N. S.; Potterton, E. A.; Powell, H. R.; Read, R. J.; Vagin, A.; Wilson, K. S. Overview of the CCP4 suite and current developments. *Acta Cryst.* **2011,** *D67*, 235-242.

42. Adams, P. D.; Afonine, P. V.; Bunkóczi, G.; Chen, V. B.; Davis, I. W.; Echols, N.; Headd J. J.; Hung, L. W.; Kapral, G. J.; Grosse-Kunstleve, R. W.; McCoy, A. J.; Moriarty, N. W.; Oeffner, R.; Read R. J.; Richardson, D. C.; Richardson, J. S.; Terwilliger, T. C.; Zwart, P. H. PHENIX: A comprehensive Python-based system for macromolecular structure solution. *Acta Cryst.* **2010,** *D66*, 213-221.

43. Moriarty, N. W.; Grosse-Kunstleve, R. W.; Adams, P. D. electronic Ligand Builder and Optimization Workbench (eLBOW): A tool for ligand coordinate and restraint generation. *Acta Cryst.* **2009,** *D65*, 1074-1080.

44. Emsley, P.; Lohkamp, B.; Scott, W. G.; Cowtan, K. Features and development of Coot. *Acta Cryst.* **2010,** *D66*, 486-501.

Figure 1.

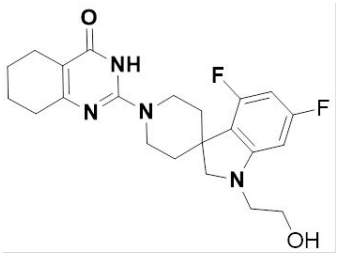

RK-287107 (**1**)

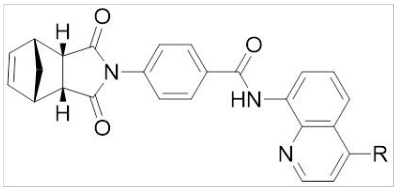

IWR-1 (R=H) (**2**)
IWR-2 (R=Me) (**3**)

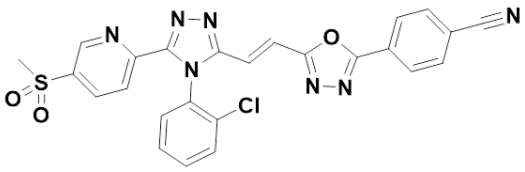

G007-LK (**4**)

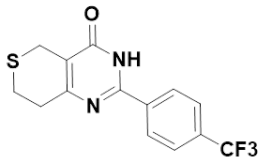

XAV-939 (**5**)

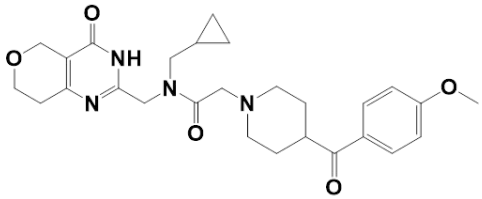

NVP-TNKS656 (**6**)

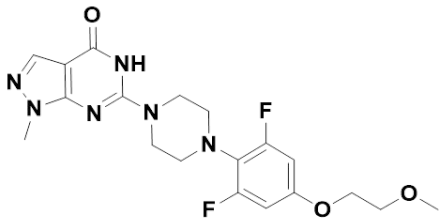

G-631 (**7**)

Figure 2.

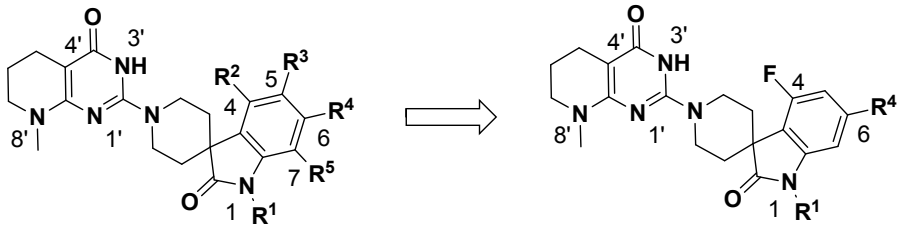

Figure 3.

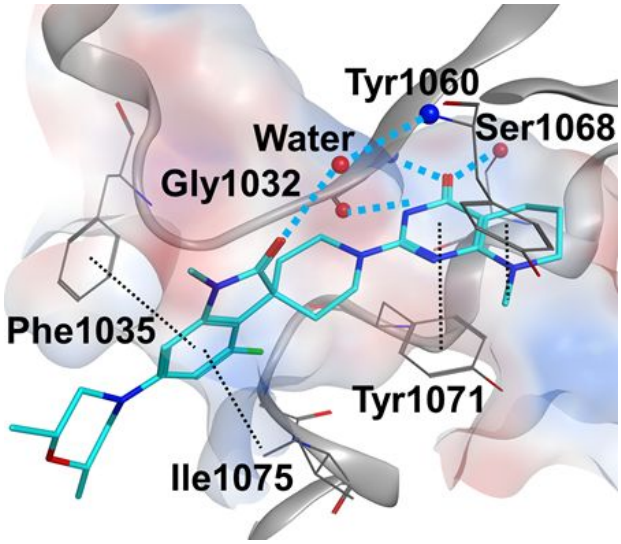

Figure 4.

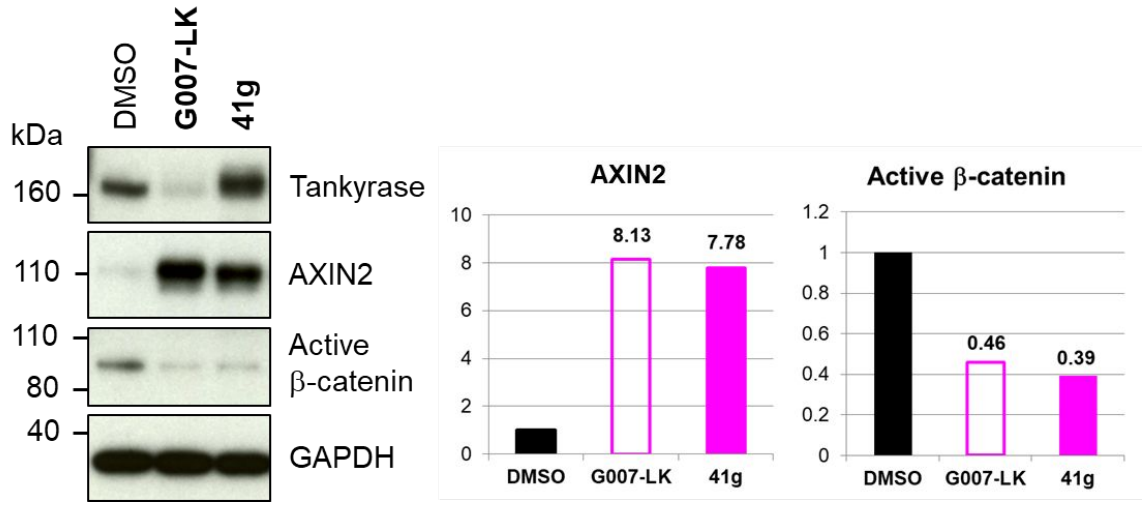

Figure 5.

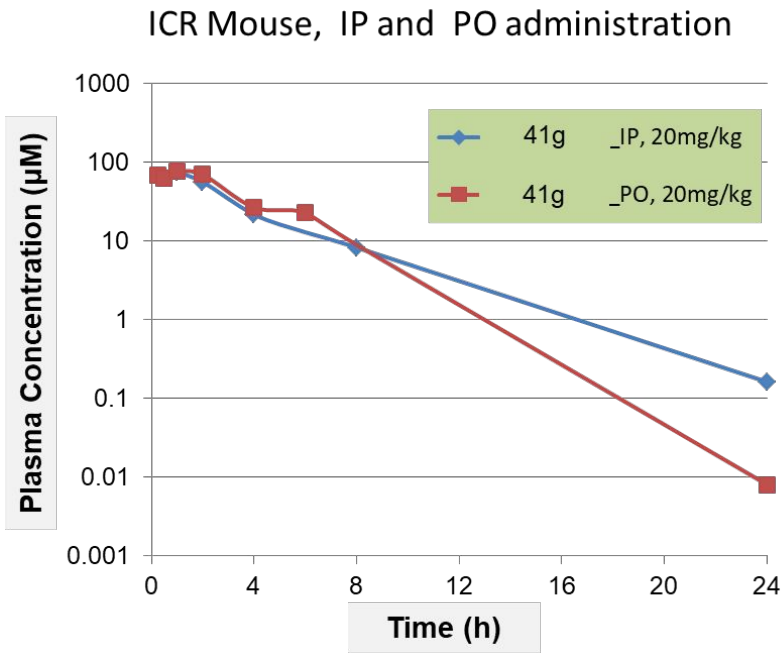
ICR Mouse, IP and PO administration
Plasma Concentration (μM)
1000
100
10
1
0.1
0.01
0.001
0
4
8
12
16
20
24
Time (h)
41g _IP, 20mg/kg
41g _PO, 20mg/kg

Figure 6.

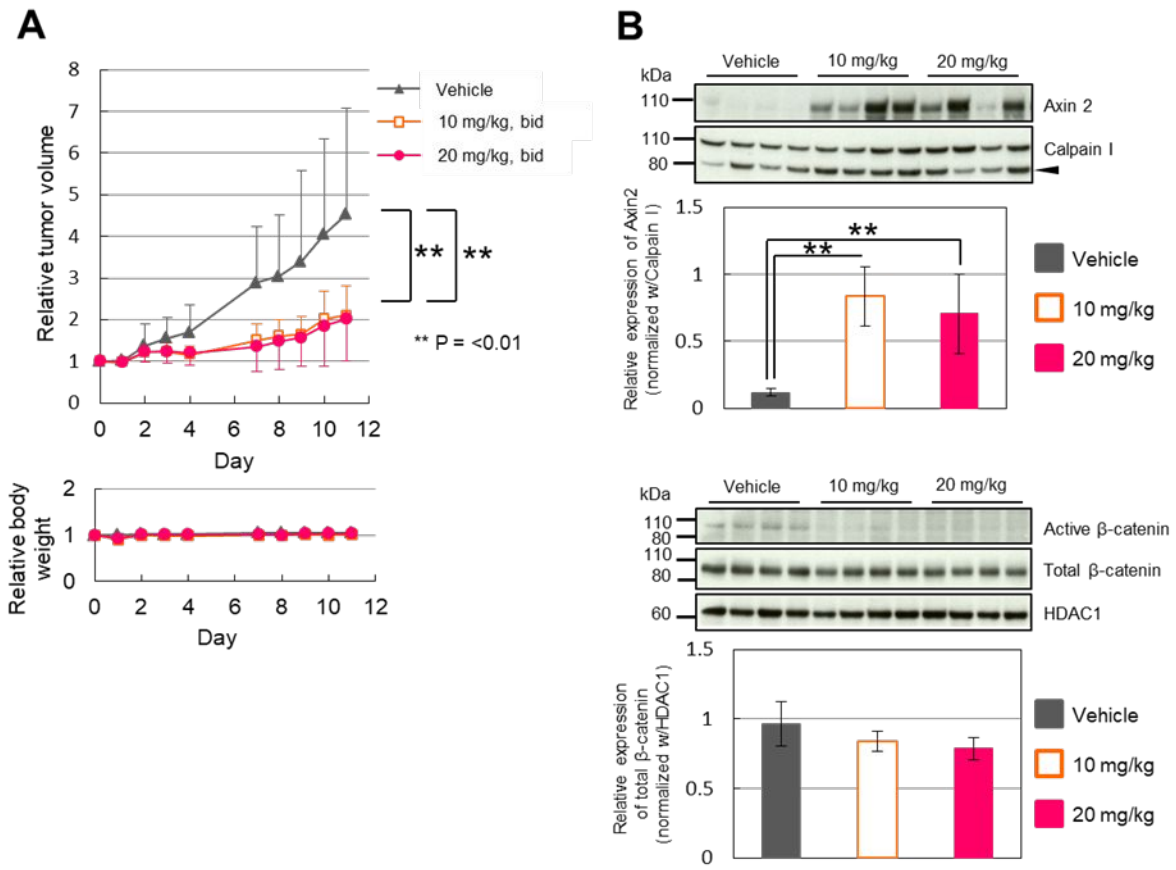
A
Relative tumor volume
Day
Vehicle
10 mg/kg, bid
20 mg/kg, bid
** P = <0.01
Relative body weight
Day
B
kDa
Vehicle
10 mg/kg
20 mg/kg
Axin 2
Calpain I
Relative expression of Axin2 (normalized w/Calpain I)
Active β-catenin
Total β-catenin
HDAC1
Relative expression of total β-catenin (normalized w/HDAC1)

Figure 7.

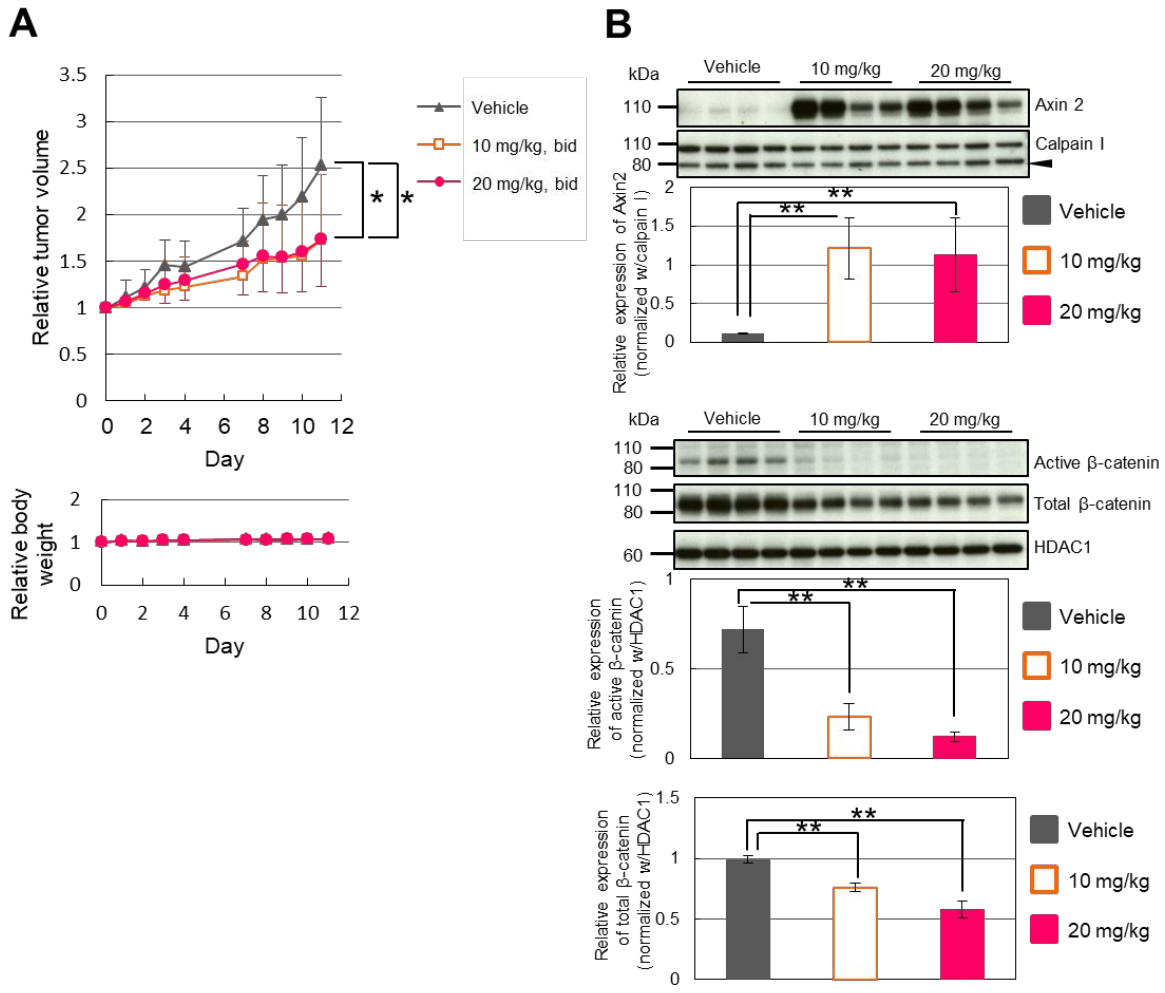
A
Relative tumor volume
Day
Vehicle
10 mg/kg, bid
20 mg/kg, bid
Relative body weight
Day
B
kDa
Vehicle
10 mg/kg
20 mg/kg
Axin 2
Calpain I
Relative expression of Axin2 (normalized w/calpain I)
Active β-catenin
Total β-catenin
HDAC1
Relative expression of active β-catenin (normalized w/HDAC1)
Relative expression of total β-catenin (normalized w/HDAC1)

Figure 1. Selected tankyrase inhibitors reported in the literature.

Figure 2. Optimization of the substituted spiroindolinone derivatives with the MTPP moiety. For compounds with superior drug-like properties, we investigated the effects of substituents at the 1- and 6-position (R^1 and R^4) on the spiroindolinone with the MTPP moiety.

Figure 3. Co-crystal X-ray structure of **41g** and tankyrase-2. Stick representation in blue depicts compound **41g**. Blue and black dashed lines denote hydrogen bonds and π-π/CH-π interactions, respectively (PDB ID: 6KRO).

Figure 4. Western blot analysis of compound **41g** and G007-LK in cultured cells. COLO-320DM cells are treated with 0.1 μM G007-LK and **41g** for 16 h. Protein expression level is determined relative to the GAPDH protein.

Figure 5. Pharmacokinetic studies of mouse intraperitoneal and oral administration.

After intraperitoneal or oral administration of **41g** at 20 mg/kg to male ICR mouse (8 weeks old, n = 3), blood samples were collected at 5 (IP) or 6 (PO) time points (IP: t = 1, 2, 4, 8 and 24 h; PO: t = 0.5, 1, 2, 4, 6 and 24 h).

Figure 6. *In vivo* antitumor effect following intraperitoneal injection of **41g**. **A**: Tumor growth inhibition by **41g** *in vivo*. NOD-SCID mice are injected subcutaneously with COLO-320DM cells. **41g** is administered with an intraperitoneal injection using a 5-day on/2-day off regimen for 2 weeks at 10 mg/kg or 20 mg/kg twice daily. Error bar indicates standard deviation. **P < 0.01 by Dunnett's test. **B**: Xenograft tumors in (A) are collected after 4 h from the final administration. Cytoplasmic (upper panels) and nuclear (lower panels) extracts from the tumor tissues are subjected to western blot analysis. Each lane indicates a tumor derived from an independent mouse. Arrow heads are non-specific bands. **P < 0.01 by a two-sided Student's paired test.

Figure 7. *In vivo* antitumor effect following oral administration of **41g**. **A**: Tumor growth inhibition by **41g** *in vivo*. NOD-SCID mice are injected subcutaneously with COLO-

320DM cells. **41g** is administered orally using a 5-day on/2-day off regimen for 2 weeks at 10 mg/kg or 20 mg/kg twice daily. Error bar indicates the standard deviation. *P < 0.05 by Dunnett's test. **B**: Xenograft tumors in (A) are collected 4 h after the final administration. Cytoplasmic (upper panels) and nuclear (lower panels) extracts from the tumor tissues are subjected to western blot analysis. Each lane indicates a tumor derived from an independent mouse. Arrow heads are non-specific bands. ** P < 0.01 by two-sided Student's paired test.

Scheme 1. Synthesis of analogs of tetrahydroquinazolinone.[a]

[a]Reagents and conditions: (a) 2-amino-3-methylbenzoic acid, urea, neat, 180 °C, 1 h; (b) $POCl_3$, neat, reflux, 6 h; (c) aq. NaOH, acetonitrile, rt, 14 h; (d) triethylamine, ethanol, microwave irradiation, 150 °C, 30 min; (e) MeI, DMF, 100 °C, 3 h; (f) H_2 / PtO_2, ethanol, rt, 14 h; (g) MeI, NaH, THF, rt, 14 h; (h) aq. 2N NaOH, reflux, 14 h; (i) H_2 / Pd-C, methanol-AcOH, rt, 14 h.

Scheme 2. Synthesis of 1-substituted spiroindolinone series. [a]

[a]Reagents and conditions: (a) (1) TFA, chloroform, reflux, 3 h; (2) *m*CPBA, rt, 1 h; (b) (**25a**-**e**, **g**) R-X, base, DMF; (**25f**) 3-oxetane-1-methanol, DEAD, PPh_3, THF, rt, 1h; (**25h**) *tert*-butyldimethyl(oxiran-2-ylmethoxy)silane, NaH, DMF, 100 °C, 5 h;(c) H_2 / Pd-C, methanol, rt; (d) triethylamine, ethanol, microwave irradiation, 150 °C, 30 min; (e) MeI, DMF, 100 °C, 3 h; (f) H_2 / PtO_2, ethanol, rt, 14 h; (g) TIPSCl, imidazole, THF, rt, 1 h; (h) MeI, NaH, DMF, rt, 1 h; (i) TBAF, AcOH, THF, rt, 1 h.

Scheme 3. Synthesis of 6-alkoxy substituents of spiroindolinone series.[a]

[a]Reagents and conditions: (a) $Pd_2(dba)_3$, *tert*-Bu_3PHBF_4, *tert*-BuONa, dioxane, MW, 180 °C, 30 min; (b) PTSA, toluene, reflux, 1 h; (c) *tert*-butyl bis(2-chloroethyl)carbamate, NaH, DMF, 80 °C, 3 h; (d) 5N NaOH, aq. H_2O_2, DMSO, rt, overnight; (e) (1) LiH, DMF, 120 °C, 6 h; (2) MeI, rt, 1 h; (f) (1) BBr_3, DCM, rt, 14 h; (2) Boc_2O, rt, 1 h; (g) (**37b, j**) RX, base, DMF, 80 °C, 3 h; (**37c–i**): ROH, DEAD, PPh_3, THF, rt, 1 h; (h) TFA, chloroform, rt, 1 h; (i) triethylamine, ethanol, microwave irradiation, 150 °C, 30 min.

Scheme 4. Synthesis of the 6-position heterocyclic substituents of the spiroindolinone series.[a]

[a]Reagents and conditions: (a) Tf_2O, triethylamine, chloroform, rt, 1 h; (b) HNR_2, $Pd(OAc)_2$, BINAP, Cs_2CO_3, toluene, reflux, 14 h; (c) TFA, chloroform, rt, 1 h; (d) triethylamine, ethanol, microwave irradiation, 150 °C, 30 min; (e) (1) $HNMe_2$, tBuONa, $Pd_2(dba)_2$, BINAP, toluene, microwave irradiation, 100 °C, 1 h; (2) H_2 / $Pd(OH)_2$-C, ethanol-dichloromethane, rt, 24 h.

Shirai *et al.* Scheme 1.

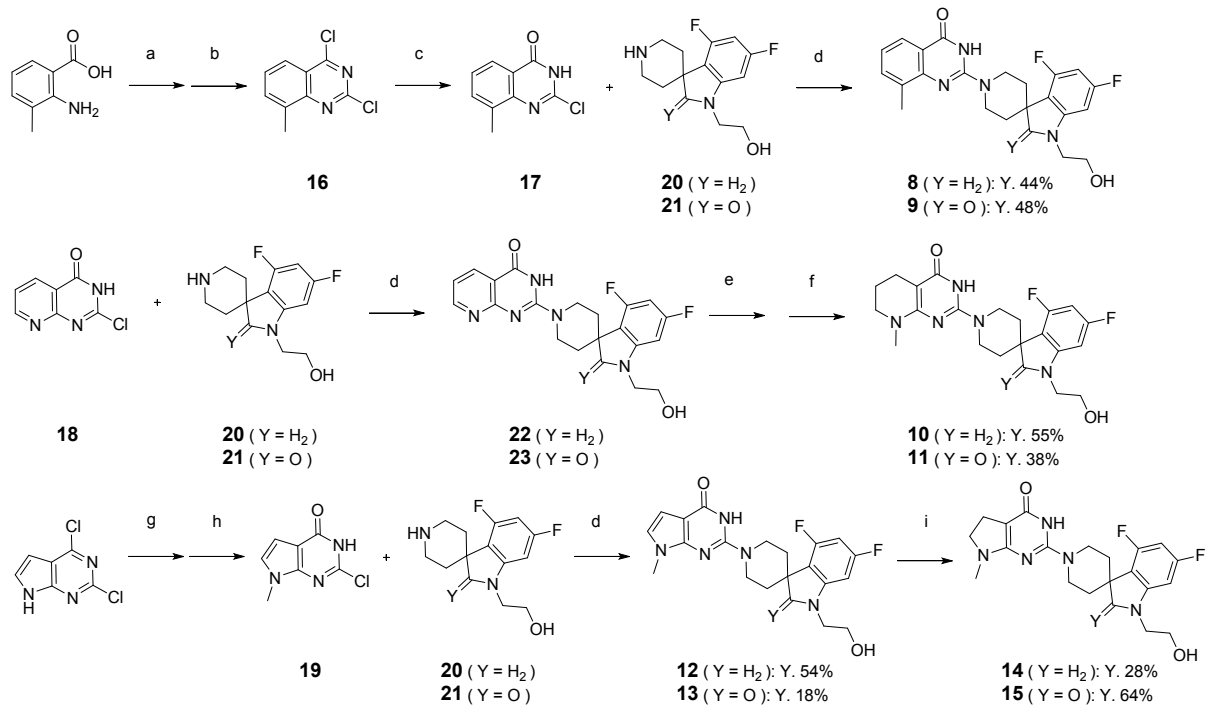

Shirai *et al.* Scheme 2.

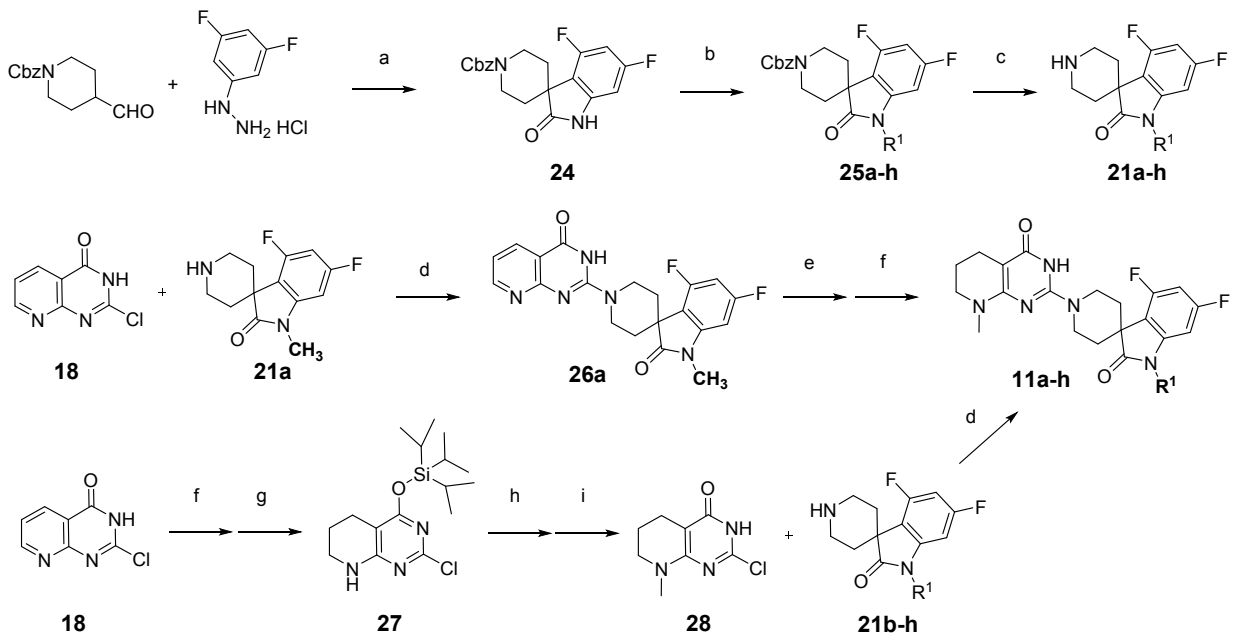

R^1 =

a: CH_3, b: $CH_2CH_2OCH_3$, c: CH_2CF_3 d: CH_2CN, e: $CH_2SO_2CH_3$, f:  g: CH_2CO_2H, h: $CH_2CH(OH)CH_2OH$

Shirai *et al.* Scheme 3.

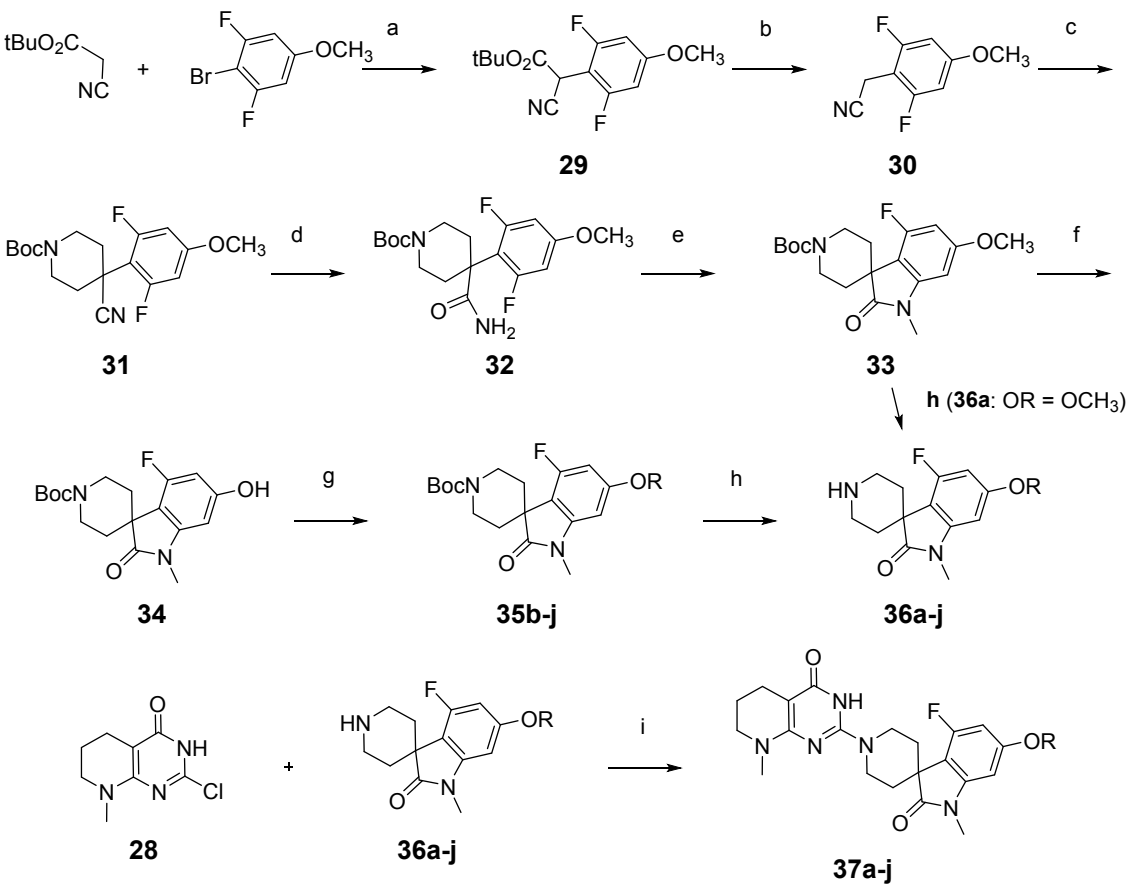

Shirai *et al.* Scheme 4.

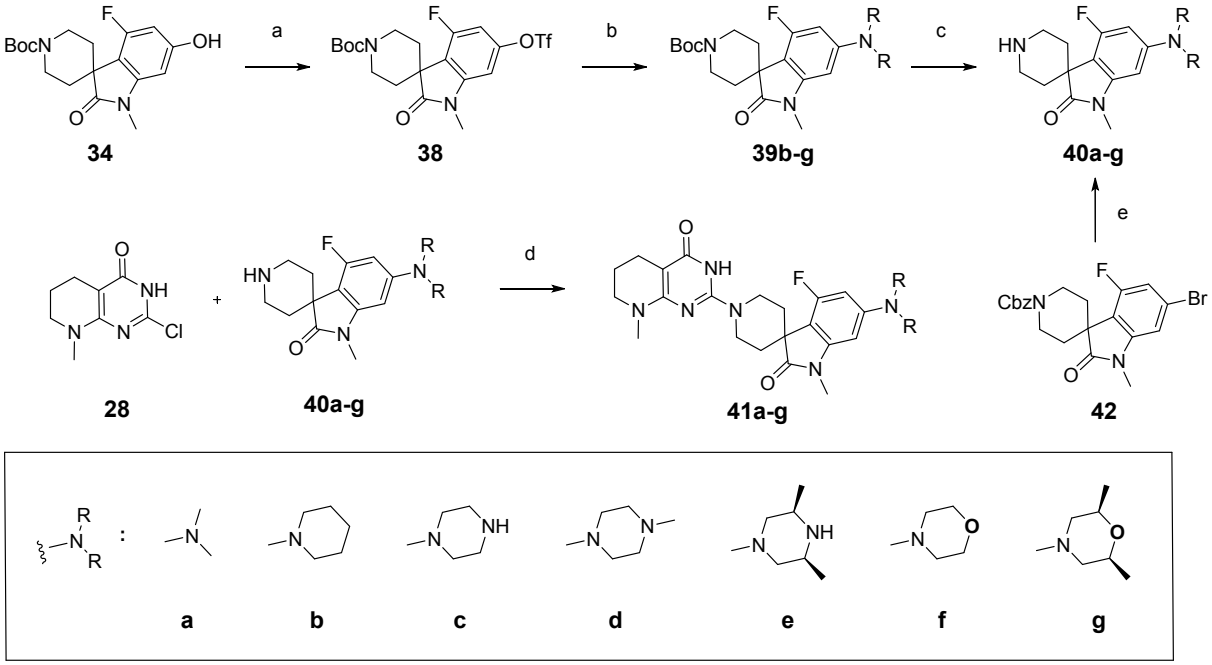

Shirai *et al.* Table of Contents graphic

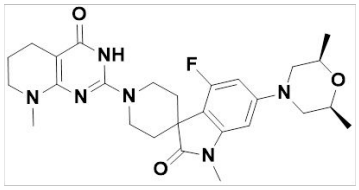

RK-582

Tankyrase-1: IC_{50} = 36.1 nM
PARP1: IC_{50} = 18 187 nM
COLO-320DM: GI_{50} = 0.23 μM